SEVENTEENTH EUROPEAN ROTORCRAFT FORUM

Paper No. 91 - 76

COUPLED ROTOR/FUSELAGE VIBRATION REDUCTION USING MULTIPLE FREQUENCY BLADE PITCH CONTROL

I. PAPAVASSILIOU, P.P. FRIEDMANN, C.VENKATESAN

MECHANICAL, AEROSPACE AND NUCLEAR ENGINEERING DEPARTMENT
UNIVERSITY OF CALIFORNIA AT LOS ANGELES
LOS ANGELES, CA 90024-1597, U.S.A

SEPTEMBER 24 - 26, 1991

BERLIN, GERMANY

Deutsche Gesellschaft fur Luft- und Raumfahrt e.v. (DGLR)

Gedesberger Allee 70, 5300 Bonn 2, Germany

COUPLED ROTOR-FUSELAGE VIBRATION REDUCTION WITH MULTIPLE FREQUENCY BLADE PITCH CONTROL

I.Papavassiliou[1] ,
P.P.Friedmann[2] and C.Venkatesan[3].
Mechanical, Aerospace, and Nuclear Engineering Department
University of California, Los Angeles, CA 90024

Abstract

A nonlinear coupled rotor/flexible fuselage analysis has been developed and used to study the effects of higher harmonic blade pitch control on the vibratory hub loads and fuselage acceleration levels. Previous results, obtained with this model have shown that conventional higher harmonic control (HHC) inputs aimed at hub shear reduction cause an increase in the fuselage accelerations and vise-versa. It was also found that for simultaneous reduction of hub shears and fuselage accelerations, a pitch input representing a combination of two higher harmonic components of different frequencies was needed. Subsequently, it was found that this input could not be implemented through a conventional swashplate. This paper corrects a mistake originally made in the representation of the multiple frequency pitch input and shows that such a pitch input can be only implemented in the rotating reference frame. A rigorous mathematical solution is found, for the pitch input in the rotating reference frame, which produces simultaneous reduction of hub shears and fuselage acceleration. New insight on vibration reduction in coupled rotor/fuselage systems is obtained from the sensitivity of hub shears to the frequency and amplitude of the open loop HHC signal in the rotating reference frame. Finally the role of fuselage flexibilty in this class of problems is determined.

Nomenclature

a	Rotor blade lift curve slope
A_{Cx4c}, A_{Cx4s}, A_{Cy4c} A_{Cy4s}, A_{Cz4c}, A_{Cz4s}	4/rev components of the fuselage C.G accelerations
A^P	Amplitude of pitch input in Eq. (41)
b	Blade semichord
C_{d0}	Blade drag coefficient
C_w	Weight coefficient
C_x, C_y, C_z	Blade damping constants
e	Hinge offset

1 Postdoctoral Fellow
3 Professor
2 Associate Research Engineer

f_b , f_f , f_e , f_λ	Column vectors of blade, fuselage rigid body, fuselage elastic and inflow equations for equilibrium
F_{Hx4c}, F_{Hx4s}, F_{Hy4c} F_{Hy4s}, F_{Hz4c}, F_{Hz4s}	4/rev components of the vibratory hub shears
F_{0Hz4c}, F_{0Hz4s}	4/rev components of the baseline vertical hub shear
J	Performance index, Eq. (35)
N_b	Number of blades
$[P_{ER}]$	Transformation matrix, Eq. (8)
q_b , q_f , q_e , q_t	Vector of the degrees of freedom of blade, fuselage rigid body modes, fuselage elastic modes and trim variables
q_{b0}, q_{bnc}, q_{bns}	Harmonic components of blade response
q_{f0}, q_{fnc}, q_{fns}	Harmonic components of fuselage rigid body response
q_{e0}, q_{enc}, q_{ens}	Harmonic components of fuselage elastic response
$\overline{R}$	Dimensional rotor radius
R_c	Elastic coupling coefficient
$[T]$, $[T_E]$, $[T_R]$	MFPC Transfer matrices
$[W_Z]$	Weighting matrix, Eq. (35)
X_{MA}, Z_{MA}	X and Z position of the fuselage aerodynamic center measured from point M on the helicopter
X_{MC}, Z_{MC}	X and Z position of the fuselage center of mass measured from point M on the helicopter
X_{MH}, Z_{MH}	X and Z position of the rotor hub center measured from point M on the helicopter
$\{Z\}$, $\{Z_A\}$, $\{Z_F\}$	Vectors of vibratory response
$\{Z_0\}$	Vector of baseline vibrations
α_R	Fuselage attitude in pitch
β_{nC}, β_{nS}	n-th harmonic cosine and sine components of flap

	response of the blade
β_k, ζ_k, ϕ_k	The k-th blade rotating flap, lead-lag and torsional degrees of freedom
γ	Lock number
$\theta_0, \theta_{1c}, \theta_{1s}$	Blade pitch settings for equilibrium
$\theta_T(x_k)$	Blade twist distribution
θ_{pk}	Control pitch angle of kth blade
θ_{HHk}	Higher harmonic pitch input of kth blade
θ	Blade pitch input or vector of pitch inputs
$\{\theta_E\}$	Vector of pitch control inputs
$\{\theta_R\}$	Vector of pitch control inputs
$\theta_{oc}, \theta_{cc}, \theta_{sc}$	Amplitudes of cosine inputs in collective, lateral and longitudinal HHC
$\theta_{os}, \theta_{cs}, \theta_{ss}$	Amplitudes of sine inputs in collective, lateral and longitudinal HHC
$\theta_{\bar{o}c}^{p}, \theta_{\bar{o}s}^{p}, \theta_{\bar{c}c}^{p}$ $\theta_{\bar{c}s}^{p}, \theta_{\bar{s}c}^{p}, \theta_{\bar{s}s}^{p}$	Components of pitch input control vector, Eq. (5)
$\theta_{\bar{c}}^{p-1}, \theta_{\bar{s}}^{p-1}, \theta_{\bar{c}}^{p}$ $\theta_{\bar{c}}^{p}, \theta_{\bar{c}}^{p+1}, \theta_{\bar{s}}^{p+1}$	Components of pitch input control vector for frequencies p-1,p and p + 1/rev respectively
λ	Total inflow
μ	Advance ratio
$\xi f_i, \xi l_i, \xi t_i$	i-th generalized degree of freedom in flap, lag and torsion for the elastic blade
$\overline{\rho}$	Density of the air
σ	Solidity ratio $= \frac{2N_b b}{\pi}$
ϕ^p	Phase angle of pitch input in Eq. (41)
ψ_k	Azimuth angle of the k-th blade

ω_{F1}, ω_{L1}, ω_{T1}	Rotating first flap, lag, and torsional blade frequencies
$\overline{\omega}_{HH}$	Frequency of the HHC input
Ω	Rotor R.P.M
$\overline{(\ )}$	Overbars indicate dimensional quantities

1. Introduction

Vibration reduction is one of the central problems in modern helicopter design. Among the various schemes available for vibration reduction [1,2] vibration reduction using higher harmonic control (HHC) appears to have considerable promise. The higher harmonic blade pitch control can be implemented either through the use of actuators in the nonrotating frame (i.e. below the the swashplate) or in the rotating frame, with actuators between the swashplate and the rotor blade. The second approach based on actuators in the rotating system is denoted Individual-Blade-Control (IBC) [3]. With the constraint that all the blades in the rotor must perform identical motion, the use of actuators in the nonrotating frame imposes limitations on the frequencies of the higher harmonic blade pitch angle which can be implemented in practice. These restrictions can be removed by using actuators in the rotating frame [4].

Vibration reduction using HHC has been demonstrated by analytical simulation [5-10] ,wind tunnel tests [11-13] and flight tests [14-16]. The analytical studies and wind tunnel tests have shown that under a fixed hub condition, the use of high frequency blade pitch inputs (HHC) reduces hub loads. It should be noted that the purpose of the analytical and wind tunnel studies was not only to assess the effectiveness of various control algorithms for HHC but also to demonstrate the technical feasibility of the approach. On the other hand, flight tests have demonstrated fuselage vibration (usually acceleration levels at the pilot seat) reduction by using HHC inputs to the main rotor. In some flight tests it was observed that reduction of acceleration components at the pilot seat was accompanied by increases in hub and blade loads from their baseline values.

In a number of recent studies [17-19] it was shown that for a coupled rotor/flexible fuselage model, shown schematically in Fig. 1, conventional single frequency higher harmonic pitch control applied through a conventional swashplate was capable of reducing either the hub loads or the fuselage accelerations but not both simultaneously. A simultaneous reduction of both hub shears and fuselage accelerations could be obtained only when assuming that the fuselage was rigid.

In an attempt to obtain simultaneous reduction of hub shears fuselage accelerations for a flexible fuselage a pitch input consisting of two different frequencies was considered. To distinguish between this input and convetional HHC, in Refs. 17-19 this input was denoted as Multiple Higher Harmonic Control(MHHC). This approach was based on employing two higher harmonic pitch inputs with frequencies of $(N_b - 1)$ /rev and (N_b) /rev for a rotor having N_b blades. Subsequently

the authors found that this pitch input used, in the previous studies [17 – 19], was incorrect; in the sense that it could not be mechanically implemented through a conventional swashplate which uses actuators in the nonrotating reference frame. As will be shown in this paper, the pitch input found in Refs. 17-19 can be implemented by using actuators in the rotating reference frame, and therefore its practical implementation can be categorized as individual blade control(IBC). Furthermore to avoid any misconception created in our previous studies, the use of pitch control inputs which consist of more than one frequency in the rotating reference will be denoted in this paper as Multiple Frequency Pitch Control (MFPC).

It turned out that the use of such multiple frequency pitch inputs, in the open loop mode, has very interesting properties, which enhance our understanding of vibration reduction in rotorcraft using HHC or any other type of actively controlled pitch input. A fairly detailed study was conducted to analyze the vibration reduction capability of such pitch inputs, using a nonlinear coupled rotor/flexible fuselage model of a helicopter in forward flight which was developed in Refs. 17-19. The mathematical model for the system schematically shown in Fig. 1, was derived using computer algebra implemented on a symbolic computing facility and the details of the derivation can be found in Refs. 17-19.

The main objectives of this study are:

1. To correct the error made in the previous studies [17-19] associated with the application of multiple frequency pitch control inputs to the coupled rotor/flexible fuselage system;
2. To provide an improved understanding of the effect of the open loop HHC inputs on a coupled rotor/fexible fuselage system by studying the sensitivity of such a system to higher harmonic blade pitch inputs, applied in the rotating system, one frequency at a time;
3. To undestand the fundamental mechanism of simultaneous reduction of hub shears and fuselage accelerations using MFPC ;
4. To study the influence of fuselage modeling on the capability of MFPC to produce simultaneous reduction in hub shears and fuselage accelerations.

2. Coupled Rotor/Flexible Fuselage Model

The first step in studying the vibration problem in helicopters is the formulation of the nonlinear differential equations of motion representing the dynamics of the coupled rotor-flexible fuselage system in forward flight. Due to the complexity of the problem, certain simplifying assumptions have been made in the idealization of the rotor-fuselage system.

A schematic diagram of the coupled rotor-fuselage system is shown in Fig. 1. The mathematical model which has been developed can accomodate two different blade models: (a) the offset hinged spring restrained blade model and (b) the fully elastic hingeless blade model. For both cases, the blades have fully coupled flap-lag- torsional dynamics. The fuselage is idealized as a uniform beam having bending deformations in the vertical and horizontal planes and elastic torsion about the $\hat{x}_1$ axis. In addition to the elastic deformations, the fuselage has five rigid body degrees of freedom namelly, pitch, roll and three translations. The rotor system is connected to the flexible beam through a rigid shaft at point "D".

The equations of motion of the coupled rotor-flexible fuselage system are derived using force and moment equilibrium conditions. For the offset hinged, spring restrained blade case the rotor blade equations are obtained by enforcing moment equilibrium at the root of the blade in flap lag and torsion. For the elastic blade case the equations are the nonlinear partial differential equations of an elastic beam. These equations are transformed to a system of ordinary nonlinear differential equations using Galerkin's method to eliminate the spatial variable. The final system of equations of motion describing the coupled flap-lag-torsional motion of the elastic blade consists of three flap equations corresponding to the first three bending modes in flap; two lag equations corresponding to the first two bending modes in lead-lag; and one torsional equation corresponding to the fundamental torsional mode. The rigid body equations of motion of the fuselage are obtained using force and moment equilibrium at the center of gravity(C.G) of the fuselage; and the elastic mode equations of the fuselage are formulated using generalized force and moment equilibrium for the various generalized modes representing the elastic deformation of the fuselage.

The details of the derivation of the equations on a symbolic computing facility can be found in Refs. 17-19.

3. Blade Pitch Representation for Open Loop Control

The total pitch angle in the rotating frame consists of two contributions; those needed to trim the helicopter and the higher harmonic pitch inputs used for vibration reduction. The pitch angle of the k-th rotor blade in the rotating frame can be expressed as:

$$\theta_{pk} = \theta_0 + \theta_{1c} \cos\psi_k + \theta_{1s} \sin\psi_k + \theta_{HHk} \tag{1}$$

where ψ_k is the blade azimuth angle of the k-th blade:

$$\psi_k = \psi + \frac{2\pi}{N_b}(k-1) \quad ; \; k = 1, 2, \ldots, N_b \tag{2}$$

Where θ_0, θ_{1c},and θ_{1s} are the collective and cyclic pitch inputs required for trim, and θ_{HHk} the higher harmonic pitch input. For HHC through a conventional swash plate, the pitch input in the rotating frame can be written:

$$\theta_{HHk} = [\theta_{OS} \sin\bar{\omega}_{HH}\psi + \theta_{OC} \cos\bar{\omega}_{HH}\psi]$$

$$+ [\theta_{CS} \sin\bar{\omega}_{HH}\psi + \theta_{CC} \cos\bar{\omega}_{HH}\psi] \cos\psi_k$$

$$+ [\theta_{SS} \sin\bar{\omega}_{HH}\psi + \theta_{SC} \cos\bar{\omega}_{HH}\psi] \sin\psi_k \tag{3}$$

The expressions inside the bracketts are the collective, lateral and longitudinal HHC inputs corresponding to translation, lateral tilting and longitudinal tilting of the stationary swashplate. To prevent the blades from going out of track, $\bar{\omega}_{HH}$ in

Eq. (3) has to be a multiple of the number of the rotor blades N_b, which results in a pitch input signal containing three frequencies, namely $(N_b - 1)$/rev, N_b/rev and $(N_b + 1)$/rev, in the rotating frame. For a four bladed rotor, $\overline{\omega}_{HH} = 4$ and the signal in the rotating frame contains only 3/rev, 4/rev and 5/rev harmonics. This imposes certain limitations in the domain of search for the signal which minimizes the vibrations. In Refs. [17-19] the HHC signal was erroneously represented by:

$$\theta_{HHk} = [\theta_{OS} \sin \overline{\omega}_{HH}\psi_k + \theta_{OC} \cos \overline{\omega}_{HH}\psi_k]$$

$$+ [\theta_{CS} \sin \overline{\omega}_{HH}\psi_k + \theta_{CC} \cos \overline{\omega}_{HH}\psi_k] \cos \psi_k$$

$$+ [\theta_{SS} \sin \overline{\omega}_{HH}\psi_k + \theta_{SC} \cos \overline{\omega}_{HH}\psi_k] \sin \psi_k \qquad (4)$$

where ψ was erroneously replaced by ψ_k in the expressions inside the square bracketts in Eq. (3). When the frequency $\overline{\omega}_{HH}$ is a multiple of the number of blades N_b , Eqns. (3) and (4) are mathematically identical. If $\overline{\omega}_{HH}$ is not a multiple of N_b, the signal given by Eq. (4) cannot be practically implemented through a conventional swashplate using actuators in the nonrotating frame. However it can be mechanically implemented by using actuators located in the rotating reference frame. The practical implementation of such a system is currently being considered by MBB [4].

For a given integer value of $\overline{\omega}_{HH}$ = p/rev the the signal given by Eq. (4) can be written as a vector with six elements:

$$\{\theta_E\} = \{\theta^p_{OC}\ \theta^p_{OS}\ \theta^p_{CC}\ \theta^p_{CS}\ \theta^p_{SC}\ \theta^p_{SS}\ \}^T \qquad (5)$$

The subscript E stands for "Error", to indicate that the input vector represented by Eq. (5) corresponds to the input signal, given by Eq. (4). Expanding Eq. (4) using trigonometric relations and collecting the harmonic contents of the signal in the rotating frame, for $\overline{\omega}_{HH}$ = p/rev, yields:

$$\theta_{HHk} = \left[\frac{1}{2}\theta^p_{CC} + \frac{1}{2}\theta^p_{SS}\right] \cos(p-1)\psi_k + \left[\frac{1}{2}\theta^p_{CS} - \frac{1}{2}\theta^p_{SC}\right] \sin(p-1)\psi_k$$

$$+ \theta^p_{OC} \cos p\psi_k + \theta^p_{OS} \sin p\psi_k$$

$$+ \left[\frac{1}{2}\theta^p_{CC} - \frac{1}{2}\theta^p_{SS}\right] \cos(p+1)\psi_k + \left[\frac{1}{2}\theta^p_{CS} + \frac{1}{2}\theta^p_{SC}\right] \sin(p+1)\psi_k \qquad (6)$$

Therefore, the pitch input represented by Eq. (4), with $\overline{\omega}_{HH}$ = p/rev , is equivalent to a pitch input consisting of three frequencies, namely (p-1)/rev, p/rev and

(p + 1)/rev, in the rotating frame. The cosine and sine components of this signal, given by Eq. (6) , can be also represented by a vector denoted as

$$\{\theta_R\} = \{\theta_C^{p-1} \;\; \theta_S^{p-1} \;\; \theta_C^{p} \;\; \theta_S^{p} \;\; \theta_C^{p+1} \;\; \theta_S^{p+1} \;\}^T \tag{7}$$

where the subscript R stands for "Rotating", to indicate that the components of the vector in Eq. (7) represent inputs provided in the rotating frame. Equation (6) provides the relationship between the vectors $\{\theta_E\}$ and $\{\theta_R\}$, which can be written in matrix form:

$$\{\theta_R\} = [P_{ER}] \; \{\theta_E\} \tag{8}$$

where the transformation matrix is given by:

$$[P_{ER}] = \begin{bmatrix} 0 & 0 & .5 & 0 & 0 & .5 \\ 0 & 0 & 0 & .5 & -.5 & 0 \\ 1 & 0 & 0 & 0 & 0 & 0 \\ 0 & 1 & 0 & 0 & 0 & 0 \\ 0 & 0 & .5 & 0 & 0 & -.5 \\ 0 & 0 & 0 & .5 & .5 & 0 \end{bmatrix} \tag{9}$$

and the inverse transformation matrix is given by:

$$[P_{RE}] = [P_{ER}]^{-1} = \begin{bmatrix} 0 & 0 & 1 & 0 & 0 & 0 \\ 0 & 0 & 0 & 1 & 0 & 0 \\ 1 & 0 & 0 & 0 & 1 & 0 \\ 0 & 1 & 0 & 0 & 0 & 1 \\ 0 & -1 & 0 & 0 & 0 & 1 \\ 1 & 0 & 0 & 0 & -1 & 0 \end{bmatrix} \tag{10}$$

Equations (8) through (10) , imply a one-to-one correspondence between the components of the vectors $\{\theta_E\}$ and $\{\theta_R\}$. This means that the six independent quantities, θ_{OC} , θ_{OS} , θ_{CC} , θ_{CS} , θ_{SC} , θ_{SS} , in Eq. (4) are associated with six independent physical quantities which represent cosine and sine components of blade pitch in-

puts in the rotating frame, as represented by Eq. (7). When two pitch inputs of the form given by Eq. (4), with two different frequencies, $\bar{\omega}_{HH}$ = p/rev and q/rev are combined, the control input vector $\{\theta_E\}$ will have a total of 12 elements, with six elements corresponding to each of the two frequencies $\bar{\omega}_{HH}$ = p/rev and q/rev respectively. When formulating the control vector $\{\theta_R\}$ in the rotating frame, using Eq. (6) and (7), the total number of elements in the vector $\{\theta_R\}$ depends on the values of the frequencies p and q/rev. If $|p-q| \leq 2$, then there is a frequency overlap in the rotating frame corresponding to p/rev and q/rev. Therefore there is no one-to-one correspondence between the two pitch control vectors $\{\theta_E\}$ and $\{\theta_R\}$, implying that the total number of elements in the vector $\{\theta_R\}$ is less than that in the vector $\{\theta_E\}$. However, if $|p-q| > 2$, then both vectors $\{\theta_E\}$ and $\{\theta_R\}$ will contain 12 elements. For a four bladed rotor, the combination of two inputs given by Eq. (4), with $\bar{\omega}_{HH}$ equal to 3/rev and 4/rev respectively, produces a pitch input with four different frequencies, namely 2/rev, 3/rev, 4/rev and 5/rev, in the rotating frame. Note that from Eq. (6), the frequency $\bar{\omega}_{HH}$ = 3/rev will produce the frequencies 2,3 and 4/rev in the rotating frame; and $\bar{\omega}_{HH}$ = 4/rev will provide the frequencies 3,4 and 5/rev in the rotating frame. After combining the terms corresponding to the common frequencies (namely 3 and 4/rev in this case) , the pitch input in the rotating frame will consist of four different harmonics which are 2, 3, 4, and 5/rev. In this case the vector $\{\theta_E\}$ will have 12 elements:

$$\{\theta_E\} = \{\theta^3_{OC}\ \theta^3_{OS}\ \theta^3_{CC}\ \theta^3_{CS}\ \theta^3_{SC}\ \theta^3_{SS}\ |\ \theta^4_{OC}\ \theta^4_{OS}\ \theta^4_{CC}\ \theta^4_{CS}\ \theta^4_{SC}\ \theta^4_{SS}\ \}^T \tag{11}$$

and the vector $\{\theta_R\}$ will have 8 elements:

$$\{\theta_R\} = \{\theta^2_C\ \theta^2_S\ \theta^3_C\ \theta^3_S\ \theta^4_C\ \theta^4_S\ \theta^5_C\ \theta^5_S\ \}^T \tag{12}$$

The transformation matrix $[P_{ER}]$ is an 8x12 matrix:

$$[P_{ER}] = \begin{bmatrix} 0 & 0 & .5 & 0 & 0 & .5 & 0 & 0 & 0 & 0 & 0 & 0 \\ 0 & 0 & 0 & .5 & -.5 & 0 & 0 & 0 & 0 & 0 & 0 & 0 \\ 1 & 0 & 0 & 0 & 0 & 0 & 0 & 0 & .5 & 0 & 0 & .5 \\ 0 & 1 & 0 & 0 & 0 & 0 & 0 & 0 & 0 & .5 & -.5 & 0 \\ 0 & 0 & .5 & 0 & 0 & -.5 & 1 & 0 & 0 & 0 & 0 & 0 \\ 0 & 0 & 0 & .5 & .5 & 0 & 0 & 1 & 0 & 0 & 0 & 0 \\ 0 & 0 & 0 & 0 & 0 & 0 & 0 & 0 & .5 & 0 & 0 & -.5 \\ 0 & 0 & 0 & 0 & 0 & 0 & 0 & 0 & 0 & .5 & .5 & 0 \end{bmatrix} \tag{13}$$

4. Solution for the Coupled Rotor/Fuselage Response

The procedure used for calculating the equilibrium state and the vibratory loads on the helicopter is based on a harmonic balance technique. In Ref.[20], different approaches to rotor-body coupling are discussed. In this paper, the "fully coupled equations approach" is used. Furthermore, in this study the trim state of the helicopter and the response solution are obtained in a single pass by simultaneously satisfying the trim equilibrium and the vibratory response of the helicopter for all the rotor and fuselage degrees of freedom. This is an extension of the harmonic balance technique which was initially developed for the aeromechanical stability problems, such as air resonance, in Refs. [21] and [22]. A brief description of the method is provided below. The equations of motion for the coupled rotor-flexible fuselage system can be symbolically writen as:

$$f_b(q, \dot{q}, \ddot{q}, q_t; \psi) = 0 \tag{14}$$

$$f_f(q, \dot{q}, \ddot{q}, q_t; \psi) = 0 \tag{15}$$

$$f_e(q, \dot{q}, \ddot{q}, q_t; \psi) = 0 \tag{16}$$

$$f_\lambda(q, \dot{q}, \ddot{q}, q_t; \psi) = 0 \tag{17}$$

The vector f_b represents the flap,lag and torsional blade equations. The vector f_f represents the fuselage rigid body motion equations. The vector f_e represents the fuselage elastic deformation equations. Finally, f_λ represents the inflow equation. The trim solution is the vector q_t , representing the quantities λ, θ_0, θ_{1c}, θ_{1s} and α_R . The response solution represented by q , consists of the following :

$$q = \begin{bmatrix} q_b \\ q_f \\ q_e \end{bmatrix} \tag{18}$$

The vector q_b, for the case of the offset hinged spring restrained blade, contains the blade degrees of freedom β_k, ζ_k, and ϕ_k , and the generalized coordinates ξf_1, ξf_2, ξf_3, ξl_1, ξl_2 and ξt_1 , for the case of elastic blade model. The vector q_f consists of the five fuselage degrees of freedom R_{Mx}, R_{My}, R_{Mz}, θ_x, θ_y. The fuselage yaw degree of freedom is not considered in the present analysis. The vector q_e represents the generalized displacements ξ_i of the fuselage elastic modes. In forward flight a periodic solution in the form of Fourier series is assumed:

$$q_b = q_{b0} + \sum_{n=1}^{N_{Hb}} q_{bnc} \cos n\psi_k + q_{bns} \sin n\psi_k \tag{19}$$

$$q_f = q_{f0} + \sum_{n=1}^{N_{Hf}} q_{fnc} \cos nN_b\psi + q_{fns} \sin nN_b\psi \tag{20}$$

$$q_e = q_{e0} + \sum_{n=1}^{N_{He}} q_{enc} \cos nN_b\psi + q_{ens} \sin nN_b\psi \tag{21}$$

where N_{Hb}, N_{Hf}, N_{He} represent the number of harmonics for the blade, fuselage rigid body and fuselage elastic mode response, respectively.

It is known that only those components of the loads that are integer multiples of the rotor passage frequency $n \times N_b$ will be transmitted to the fuselage through the rotor hub. Hence the response of the fuselage rigid body and elastic degrees of freedom contains only integer multiples of N_b per rev harmonics. The vibratory response of the fuselage rigid body degrees of freedom was evaluated about an equilibrium state. Hence the constant pitch and roll attitudes of the fuselage are not included in the response expressions and they appear only in the trim vector q_t . The substitution of equations Eqs. (19) - (21) in equations Eqs. (14) - (17) combined with the harmonic balance technique yields a system of nonlinear coupled algebraic equations. Solution of the nonlinear algebraic system is obtained using a Newton algorithm.

5. Vibration Reduction Using Open Loop Pitch Control

In vibration reduction schemes using higher harmonic blade pitch control, the nonlinear relationship between the Multiple Frequency Pitch Control (MFPC) inputs and the vibration outputs is usually represented by a linear quasi- steady matrix relationship, in frequency domain. The input control vector $\{\theta\}$ consists of sine and cosine components of the harmonic pitch inputs and the output vector $\{Z\}$ consists of sine and cosine components of the steady state vibratory loads and accelerations. In representing a linear relation between the pitch control vector and the vibration vector, two models can be formulated; they are: (a) a local model and (b) a global model [23,24].

The local model is essentially a linearization about the current step, while the global model represents a linearization about the baseline uncontrolled vibration level. The local model can be represented as

$$\{Z(i)\} = \{Z(i-1)\} + [T](\{\theta(i)\} - \{\theta(i-1)\}) \tag{22}$$

This equation can also be written as

$$\{Z(i)\} - \{Z(i-1)\} = [T](\{\theta(i)\} - \{\theta(i-1)\})$$

or

$$\{\Delta Z(i)\} = [T]\{\Delta\theta(i)\} \tag{23}$$

In this local model, the transfer matrix [T] relates the change in vibratory response $\{Z(i)\} - \{Z(i-1)\}$ due to an increment in the higher harmonic control input $\{\theta(i)\} - \{\theta(i-1)\}$ evaluated at the current control step. In the local model, the transfer matrix [T] is treated as a function of the control input vector $\{\theta\}$ therefore at every step i, the [T] matrix is re-evaluated. In the present study on vibration reduction using open loop MFPC, the index i in Eqns. (22) or (23) represents the computational iteration step, for updating the higher harmonic control pitch input. During each iteration step, the coupled rotor/fuselage nonlinear equations are solved with the control input evaluated in the previous iteration to obtain the vibration vector $\{Z(i-1)\}$. If the vibration reduction is not satisfacory (i.e., if the fuselage vibration levels are greater than 0.005g), the transfer matrix [T] is updated about the current control input and using a suitable control scheme (two control schemes are described in the next two sections), the new control input is evaluated and this process is repeated until the criterion for the reduction in fuselage acceleration levels is met. In the computational program, every iteration is initiated externally. Therefore, the analyst can also terminate the iteration process at any stage, even if the convergence criterion is not satisfied.

In the global model, the relation between the vibratory response and the harmonic pitch input is represented by

$$\{Z(i)\} = \{Z_0\} + [T]\{\theta(i)\} \tag{24}$$

where $\{Z_0\}$ represents the baseline uncontrolled vibration level. The transfer matrix [T] in the global model, is treated as a constant and it is evaluated about the baseline case with zero higher harmonic control input. In the present study, a local model is used for vibration reduction.

5.1 Vibration minimization with pitch input $\{\theta_E\}$

The multi- frequency higher harmonic pitch control input for the k-th blade, as given by Eq. (4), consisting of a combination of two pitch inputs with frequencies $\bar{\omega}_{HH} = 3$/rev and 4/rev respectively, can be written as

$$\theta_{HHk} = [\theta^3_{OS} \sin 3\psi_k + \theta^3_{OC} \cos 3\psi_k]$$

$$+ [\theta^3_{CS} \sin 3\psi_k + \theta^3_{CC} \cos 3\psi_k] \cos \psi_k$$

$$+ [\theta^3_{SS} \sin 3\psi_k + \theta^3_{SC} \cos 3\psi_k] \sin \psi_k$$

$$+ [\theta^4_{OS} \sin 4\psi_k + \theta^4_{OC} \cos 4\psi_k]$$

$$+ [\theta^4_{CS} \sin 4\psi_k + \theta^4_{CC} \cos 4\psi_k] \cos \psi_k$$

$$+ [\theta^4_{SS} \sin 4\psi_k + \theta^4_{SC} \cos 4\psi_k] \sin \psi_k \qquad (25)$$

where the superscript 3 and 4 refer to the amplitudes of the pitch components corresponding to the harmonic frequencies $\bar{\omega}_{HH} = 3$/rev and 4/rev, respectively. The pitch input represented by Eq. (25) can be written as a control vector $\{\theta_E\}$, having 12 elements as defined below.

$$\{\theta_E\} = \{\theta^3_{OC}\ \theta^3_{OS}\ \theta^3_{CC}\ \theta^3_{CS}\ \theta^3_{SC}\ \theta^3_{SS}\ |\ \theta^4_{OC}\ \theta^4_{OS}\ \theta^4_{CC}\ \theta^4_{CS}\ \theta^4_{SC}\ \theta^4_{SS}\ \}^T \qquad (26)$$

A local model is obtained by using Eq. (23) to relate the pitch control vector $\{\theta_E\}$ to twelve components of the vibratory response of the coupled rotor/ fuselage system which are selected in an appropriate manner. From the solution of the coupled rotor/fuselage response problem, the components of hub shears and hub moments as well as the linear acceleration components at a particular location in the fuselage (such as C.G) are available in three orthogonal directions. One of the objectives of this study is the simultaneous minimization of the sine and cosine components of the 4/rev hub shears together with the 4/rev fuselage acceleration at the C.G. For this particular case, the vibration vector $\{Z\}$ is defined as

$$Z = \{Z_F^T\ \ Z_A^T\}^T \qquad (27)$$

where the vector of hub shears Z_F and the vector of C.G. accelerations Z_A are defined as:

$$Z_F = \{F_{Hx4c}\ F_{Hx4s}\ F_{Hy4c}\ F_{Hy4s}\ F_{Hz4c}\ F_{Hz4s}\}^T \qquad (28)$$

$$Z_A = \{A_{Cx4c}\ A_{Cx4s}\ A_{Cy4c}\ A_{Cy4s}\ A_{Cz4c}\ A_{Cz4s}\}^T \qquad (29)$$

The local model relating the control vector $\{\theta_E\}$ and the vibration vector $\{Z\}$ can be written as

$$\{Z(i)\} = \{Z(i-1)\} + [T_E]\,(\{\theta_E(i)\} - \{\theta_E(i-1)\}) \qquad (30)$$

This equation can also be written as

$$\{Z(i)\} - \{Z(i-1)\} = [T_E]\,(\{\theta(i)\} - \{\theta(i-1)\})$$

The subscript E implies that the 12x12 transfer matrix $[T_E]$ corresponds to the pitch control vector $\{\theta_E\}$. When this approach is implemented in a computational scheme for vibration reduction, the matrix $[T_E]$ is evaluated numerically by a finite difference procedure, at every iteration step i. In every iteration, each column of the $[T_E]$ matrix is evaluated by using a small increment of 0.005 rad for the corresponding component of the current control input vector $\{\theta_E\}$ and calculating the resulting changes in the 4/rev components of the hub shears and the fuselage accelerations. The four columns of the $[T_E]$ matrix corresponding to the control inputs θ^3_{OC} , θ^3_{OS} , θ^4_{OC} and θ^4_{OS} are obtained from the vibratory response, of the coupled rotor/fuselage system, to a single frequency harmonic input; i.e., 3/rev for θ^3_{OC} , θ^3_{OS} and 4/rev for θ^4_{OC} , θ^4_{OS} . The remaining 8 columns of the transfer matrix $[T_E]$ corresponding to the eight control inputs θ^3_{CC} , θ^3_{CS} , θ^3_{SC} , θ^3_{SS} , θ^4_{CC} , θ^4_{CS} , θ^4_{SC} and θ^4_{SS} are obtained from the response of the rotor/fuselage system to a pitch control input having two frequencies. This is evident from examining the pitch control input in Eq. (25) corresponding to these eight elements. For example, the pitch input θ_{HHk} corresponding to θ^3_{CC} is $\theta^3_{CC} \cos 3\psi_k \cos \psi_k$ which can be written as a sum of harmonics as $0.5\, \theta^3_{CC}[\cos 4\psi_k + \cos 2\psi_k]$. The column of the $[T_E]$ matrix corresponding to the element θ^3_{CC} is evaluated by providing a small increment of 0.005 rad to θ^3_{CC} and calculating the resulting changes in the 4/rev loads, from the nonlinear coupled rotor/fuselage equations. Since the input consists two frequencies, namely 2/rev and 4/rev, it is evident that the column of $[T_E]$ corresponding to the element θ^3_{CC} is obtained from the response of the nonlinear system to an input having two harmonic frequencies.

At each iteration step, the multi-frequency pith control input $\{\theta_E\}$ required for simultaneous reduction of hub shears and fuselage accelerations, is obtained by setting $Z(i) = 0$ in Eq. (30) and solving for $\{\theta_E(i)\}$ using the following relation

$$\{\theta_E(i)\} = \{\theta_E(i-1)\} - [T]^{-1} \{Z(i-1)\} \tag{31}$$

When the iteration is started, $i = 1$, corresponds to the baseline case without the control input $\{\theta_E\}$ i.e., $\{\theta_E(0)\} = 0$ and $\{Z(0)\}$ represents the baseline uncontrolled vibration vector. Note that in this procedure the control vector $\{\theta_E\}$ can be formulated only when the transfer matrix $[T_E]$ (which is a 12x12 matrix) has an inverse.

5.2 Vibration minimization with pitch input $\{\theta_R\}$

An alternative and more straightforward approach to this vibration minimization problem can be obtained by using directly the pitch control input provided in the rotating frame. The multi-frequency pitch control input θ_{HHk} in the rotating frame can be represented as a sum various harmonics. In this study, the pitch input is assumed to consist of four frequencies, namely, 2,3,4 and 5/rev; which can be mathematically represented as

$$\theta_{HHk} = \theta^2_C \cos 2\psi_k + \theta^2_S \sin 2\psi_k$$

$$+ \theta_C^3 \cos 3\psi_k + \theta_S^3 \sin 3\psi_k$$

$$+ \theta_C^4 \cos 4\psi_k + \theta_S^4 \sin 4\psi_k$$

$$+ \theta_C^5 \cos 5\psi_k + \theta_S^5 \sin 5\psi_k \tag{32}$$

where superscripts 2,3,4 and 5 refer to the frequencies 2,3,4 and 5/rev, respectively.

For this case, the control input vector $\{\theta_R\}$ consists of 8 elements and is given by

$$\{\theta_R\} = \{\theta_C^2 \ \theta_S^2 \ \theta_C^3 \ \theta_S^3 \ \theta_C^4 \ \theta_S^4 \ \theta_C^5 \ \theta_S^5 \ \}^T \tag{33}$$

The local control model, relating the 8 elements of the control vector $\{\theta_R\}$ to the 12 elements of the vibration vector $\{Z\}$ can be written as

$$\{Z(i)\} = \{Z(i-1)\} + [T_R](\{\theta_R(i)\} - \{\theta_R(i-1)\}) \tag{34}$$

In Eq. (34) the transfer matrix $[T_R]$ is a rectangular matrix of size 12x8. In this case, the procedure adopted for calculating the vector $\{\theta_R\}$ required for simultaneous reduction of hub loads and fuselage accelerations, is based on a minimum variance control algorithm employing the deterministic controller approach [23,24]. The minimum variance control algorithm is based on minimizing a performance index, which in our case, can be simply stated as

$$J = \{Z(i)\}^T [W_Z] \{Z(i)\} \tag{35}$$

where $[W_Z]$ is a weighting matrix. Imposing the condition

$$\frac{\partial J}{\partial \{\theta_R(i)\}} = 0 \tag{36}$$

and using the local linear model, given in Eq. (34), the control input vector $\{\theta_R\}$ can be obtained from

$$\{\theta_R(i)\} = -[D][T_R]^T [W_Z](\{Z(i-1)\} - [T_R]\{\theta_R(i-1)\})$$

$$\text{where } D = \left[[T_R]^T [W_Z][T_R]\right]^{-1} \tag{37}$$

In the present study, the weighting matrix $[W_Z]$ is taken as a unit matrix. Thus, the performance index essentially represents the sum of the squares of the 4/rev sine and cosine components of the hub shears and fuselage accelerations. When the

index i in Eq. (34) has a value i = 1, it corresponds to the baseline case with zero values for the pitch control input $\{\theta_R\}$. This deterministic controller approach is a simplified version of the control methodology described in Refs. 23 and 24.

In every iteration, each column of the $[T_R]$ matrix is evaluated by using a small increment of 0.005 rad for the corresponding component of the current control input vector $\{\theta_R\}$ and calculating the resulting changes in the 4/rev components of the hub shears and the fuselage accelerations. The eight columns of the $[T_R]$ matrix corresponding to the eight control inputs θ_C^2 , θ_S^2 , θ_C^3 , θ_S^3 , θ_C^4 , θ_S^4 , θ_C^5 and θ_S^5 are obtained from the responses, of the coupled rotor/fuselage system, to a single frequency harmonic input applied one at a time. This approach differs somewhat from that used in the evaluation of some of the columns of the $[T_E]$ matrix, described in the previous section. Recall that 8 columns of the $[T_E]$ matrix were obtained using control inputs which consisted of a combination of two harmonic frequencies.

5.3 Relation between the transfer matrices $[T_R]$ and $[T_E]$

Since there is a linear relationship between the MFPC inputs, represented by the vectors $\{\theta_E\}$ and $\{\theta_R\}$, a relationship between the $[T_E]$ and $[T_R]$ matrices corresponding to these vectors can also be obtained. The linear transformation between $\{\theta_R\}$ and $\{\theta_E\}$ can be written, using Eq. (8)

$$\{\theta_R\} = [P_{ER}]\ \{\theta_E\} \tag{38}$$

where the vector $\{\theta_E\}$ is 12x1, (Eq. 26), and the vector $\{\theta_R\}$ is 8x1, (Eq. 33), thus the transformation matrix $[P_{ER}]$ is 8x12, Eq. (13). Combining Eqs. (34) and (38) one has

$$\{Z(i)\} = \{Z(i-1)\} + [T_R]\,[P_{ER}]\,(\{\theta_E(i)\} - \{\theta_E(i-1)\}) \tag{39}$$

Comparing Eqs. (30) and (39) implies

$$[T_E] = [T_R]\,[P_{ER}] \tag{40}$$

In this relation, the transfer matrix $[T_E]$ whose size is 12x12, is formulated by multiplying two matrices $[T_R]$ and $[P_{ER}]$ whose rank is less than 12. Thus, the determinant of the matrix $[T_E]$ must be zero and hence the matrix $[T_E]$ is singular. However, in the vibration reduction calculations using the control vector $\{\theta_E\}$, the transfer matrix $[T_E]$ was evaluated following the procedure outlined in Section 5.1 and the use of Eq. (40) was bypassed. Simultaneous reduction of hub shears and fuselage accelerations based upon the pitch control vector $\{\theta_E\}$ implies the existence of the inverse of $[T_E]$. However if the matrix $[T_E]$ is singular, as implied by Eq. (40) its inverse will not exist and the method of vibration reduction based on the control vector $\{\theta_E\}$ and transfer matrix $[T_E]$, and described in Section 5.1, is doomed to fail. The vibration reduction analyses performed with the pitch control vector $\{\theta_E\}$ did not pose any numerical problem and the scheme was successful in minimizing the hub loads and fuselage accelerations simultaneously [17,18]. This

poses an apparent paradox. To fully understand the situation, a term by term comparison was made between the transfer matrix $[T_E]$ evaluated using the procedure outlined in Sec. 5.1 and the matrix $[T_E]$ based on Eq. (40). It was found that while the columns corresponding to the control inputs θ^3_{OC}, θ^3_{OS}, θ^4_{OC} and θ^4_{OS} are identical, there were differences in the remaining eight columns corresponding to the other eight control inputs θ^3_{CC}, θ^3_{CS}, θ^3_{SC}, θ^3_{SS}, θ^4_{CC}, θ^4_{CS}, θ^4_{SC} and θ^4_{SS}. The reason for this difference can be understood, if one recognizes the fact that the eight columns corresponding to the eight control inputs θ^3_{CC}, θ^3_{CS}, θ^3_{SC}, θ^3_{SS}, θ^4_{CC}, θ^4_{CS}, θ^4_{SC} and θ^4_{SS} were obtained from the responses, of the coupled rotor/fuselage nonlinear dynamic system, to a pitch control input having two harmonic frequencies. Since the equations of motion of the coupled rotor/fuselage system are nonlinear, the principle of superposition (of two inputs having different frequencies) does not hold. On the other hand the calculation of the $[T_E]$ matrix based on Eq. (40) is equivalent to evaluating the columns of the $[T_E]$ matrix by superposing the responses corresponding to each harmonic frequency; since the columns of $[T_R]$ are obtained using a single frequency harmonic input, as explained in Sec. 5.2. Therefore the transfer matrix $[T_E]$ formulated using the procedure in Sec. 5.1 is different from the $[T_E]$ matrix obtained from Eq. (40).

It will be demonstrated in the results section that for the coupled rotor/fuselage example treated in this study, the MFPC vector $\{\theta_E\}$ obtained using the procedure described in Sec. 5.1 and the control vector $\{\theta_R\}$ represent almost identical pitch variation in the rotating frame and both inputs produce simultaneous reduction in hub shears and fuselage accelerations.

6. Results and Discussion

The results presented in this paper deal with four separate items. The first part considers the problem of simultaneous reduction of hub shears and fuselage accelerations using open loop MFPC in the rotating reference frame, for coupled rotor/flexible fuselage systems. In the second part, the results of a sensitivity analysis is provided showing the behaviour of the 4/rev hub loads with respect to the frequency of the pitch control input in the rotating frame. A comparative study of the results obtained for the vibration reduction using the two control vectors $\{\theta_E\}$ and $\{\theta_R\}$ is presented, in the third section. In the final part, the results showing influence of fuselage flexibility on the simultaneous reduction of hub loads and fuselage accelerations is considered.

6.1 Vibration reduction using Multiple Frequency Pitch Control

The results presented in this portion of the paper are aimed at developing a physical undestanding for the open-loop MFPC scheme when applied to the vibration reduction problem of coupled rotor/flexible fuselage systems.

Two separate cases are considered. For the first case, the four bladed rotor is idealized as a offset hinged spring restrained blade model with coupled flap-lag-torsional dynamics for each blade. The data used for this case is presented in Table 1. For the second case, each blade of the four bladed rotor is modeled as a fully elastic hingeless blade, represented by six uncoupled rotating modes, corresponding to the first three flap, first two lag and a torsional mode. The data used for this caes is provided in Table 2.

For both cases the fuselage has five rigid body degrees of freedom combined with six elastic degrees of freedom. The fuselage elastic degrees of freedom consist of two flexible modes for bending in the vertical plane, bending in the horizontal plane and torsion along the X_1 axis, respectively.

All the results were calculated for an advance ratio of $\mu = 0.3$, unless otherwise stated. In these vibration studies, the worst possible case with a fundamental bending natural frequency in the vertical plane equal to 4/rev, was considered. Very high stiffnesses (fundamental natural frequency =3000/rev) in horizontal bending and in torsion, were assumed. This essentially implies that the fuselage flexible degrees of freedom in lateral bending and torsion are suppressed.

Figure 2 illustrates the MFPC pitch angle variation together with its harmonic contents, in the rotating frame, for the first three iterations. The MFPC control signal corresponds to the control vector $\{\theta_E\}$ with the frequencies $\overline{\omega}_{HH}$ = 3/rev and 4/rev. The first iteration case (dotted line) corresponds to the control input calculated about the baseline uncontrolled vibration level. Examination of the harmonic contents of this signal reveals that the 2/rev content has a maximum amplitude of 1 deg.; with 0.15deg., 0.003deg., and 0.0007deg., respectively in the 3,4 and 5/rev harmonic components. It can be seen from Fig. 2 that the difference between the signals corresponding to the three itrations, is very small. This implies that the control pitch input has converged to a value which provides a very good reduction in vibratory loads and accelerations, even after the first iteration.

The peak to peak values of the hub loads and fuselage C.G. accelerations for each iteration as well as the baseline values are shown in Table 3. For all practical purposes vibrations are completely suppressed after first iteration except for the hub rolling moment (MHX) for which a slight increase can be noticed in the second iteration.

Figure 3 illustrates the MFPC pitch angle variation corresponding to the control vector $\{\theta_E\}$ obtained with two different combination of frequencies namely, (1) $\overline{\omega}_{HH}$ = 3 and 4/rev and (2) $\overline{\omega}_{HH}$ = 3 and 5/rev. It can be seen from Fig. 3 that the pitch control vectors $\{\theta_E\}$ corresponding to these two cases produce almost identical pitch angle variation in the rotating frame. When considering the harmonic content associated with the 2, 3, and 4/rev components for these two control signals, it is evident that they have practically the same amplitudes. However, the amplitute of the 5/rev content is substantially greater in the case of 3 and 4/rev combination than that corresponding to the 3 and 5/rev MFPC combination. The amplitude corresponding to the 6/rev harmonic in the 3 and 5/rev MFPC signal is approximately 0.007 deg. Since the 3 and 4/rev combination MFPC signal does not contain a 6/rev harmonic component in the rotating frame, its amplitude is zero.

Figure 4 shows the baseline vibratory hub loads and the fuselage accelerations together with the controlled levels obtained with the two combinations of MFPC inputs. It can be seen from this figure that when a MFPC signal consisting of a superposition of 3 and 4/rev or 3 and 5/rev inputs is provided, the vibratory hub loads and the C.G. accelerations are reduced simultaneously.

Figure 5 shows the pitch angle variation for the MFPC in the rotating frame for three iteration steps; for the case where the blades are represented by a fully elastic blade model. The first iteration case (dotted line) corresponds to the control input calculated about the uncontrolled baseline vibration levels. A fourier analysis of

the final MFPC signal (solid line) obtained after the 2nd iteration indicates that the 2/rev harmonic content is again dominant, with 30% content in 3/rev and a 10% to 20% content in 4/rev and 5/rev.

The peak to peak values of the hub loads and the fuselage C.G. accelerations for each iteration as well as the baseline values are shown in Table 4. The effectiveness of the MFPC scheme in reducing the vertical acceleration at the fuselage C.G. is evident from this Table which indicates a reduction of 99% after the second iteration. Furthermore, it is also evident from Table 4 that the hub shears and moments are also substantially reduced.

6.2 Sensitivity of hub loads to higher harmonic pitch input

The results presented in the previous section indicate that for simultaneous reduction of hub shears and fuselage accelerations,the MFPC signal in the rotating frame appears to be composed of a predominantly 2/rev variation with very small contributions from other harmonics. The authors were intrigued by this behavior which seems to emphasize the importance of the 2/rev component. Therefore a careful sensitivity study was carried out so as to gain a better understanding of the effect of introducing a single harmonic pitch control input, in the rotating frame, on the vibratory 4/rev hub shears in a four bladed rotor. In this sensitivity study, the offset hinged spring restrained blade model was used. The data for the helicopter configuration are given in Table 1. During this sensitivity study, the fuselage was assumed to be rigid. This was achieved by setting the natural frequencies of the fuselage elastic modes to 3,000/rev.

When a single frequency pitch input, with frequency p/rev in the rotating frame, is introduced , the signal can be represented by:

$$\theta^{p}_{HHk} = A^{p} \sin(p\psi_k + \phi^{p}) \qquad (41)$$

where A^p is the amplitude and ϕ^p is the phase angle of the signal. The superscript p representing the frequency of the harmonic input can be 2,3,4 or 5/rev. Without loss of generality one can limit such a study on the cosine and sine components of the vertical hub shears F_{Hz4c} and F_{Hz4s}.

Figure 6 shows the peak to peak vertical hub shear when a pitch input of the type given by Eq. (41) is applied. The amplitude A^p was fixed at 0.0005 rad and the phase angle was varied between 0 to 360 degrees, in 60 degree increments. Four different frequencies: 2,3,4 and 5/rev were considered and the baseline case is also shown. It is evident from Fig. 6, that for a 4/rev input with an amplitude of 0.0005rad the peak to peak vertical hub shear is never reduced below its baseline value. However when the pitch inputs have frequencies of 2/rev, 3/rev and 5/rev, respectively, a reduction in vibratory vertical hub shear is achieved.

In order to gain a better understanding of the curves plotted in Fig. 6, a more comprehensive parametric study was performed. In this detailed study plots of the peak to peak vertical hub shear as a function of the phase angle ϕ^p, with the amplitude A^p as a parameter, were obtained. In order to choose the proper range of values for the amplitudes, a semi-theoretical anlysis was conducted first, so as to be able to identify the amplitude which produces a complete cancellation of the peak to peak vertical hub shear. This amplitude denoted by A^p min, is called the

"critical higher harmonic amplitude". A derivation of this amplitude is presented in Appendix A.

Figures 7 and 8 contain two series of plots each. Each series of plots depicts the effect of a single frequency pitch input, having five different amplitudes (1/2 A min, A min, 3/2 A min, 2 A min and 5/2 A min), on the peak to peak vertical hub shears. Where A min is based on the approximate value calculated from Eq. (A3), given in Appendix A. For each of these amplitudes the phase angle was varied from 0 to 360 degrees, in 60 degree increments, and the coupled rotor/fuselage computer code was used to obtain the response. In Figs. 7 and 8 only the peak to peak vertical hub shear is ploted, but similar plots can be obtained for all vibratory loads and fuselage accelerations. A comparison between the critical amplitudes A min for the frequencies 2/rev, 3/rev, 4/rev and 5/rev indicates that the peak to peak vertical hub shear is most sensitive to 4/rev input (A min = 0.00016 rad) and least sensitive to 2/rev input (A min = 0.0049 rad).

In order to verify this important behavior, which has not been emphasized in the literature before, an independent analytical sensitivity study of the vertical hub shear of a four bladed rotor system was conducted. In this simplified model, each blade was represented by a centrally hinged spring restrained blade model having only flap degree of freedom. A multiple frequency pitch input was introduced in the rotating frame. The response was obtained from the linear flap equation, using a quasi-steady aerodynamic model with time varying pitch, and neglecting reverse flow effects. A concise description of this study can be found in Appendix B. The conclusions of this analytical study confirmed and reinforced the trends shown in Figs. 7 and 8.

It is important to emphasize that amplitudes of the order of 0.00016 rad (0.00917 degrees) as in the case of 4/rev input are impossible to achieve in practice. For the 4/rev pitch input case, it is evident from Fig. 8, that when the amplitude exceeds 2 A min, vibration reduction cannot be achieved. Therefore amplitudes greater than 0.0183 degrees will result in an increase of the peak to peak vertical hub shear above the baseline value for any value of the phase angle ϕ[4].

The sensitivity of the 4/rev hub shears, to the various single frequency pitch inputs, is the basis for understanding the large 2/rev content in the MFPC signals obtained in Refs. 17-19, and shown in Figs. 2,3 and 5. Because the 2/rev pitch input is least effective in reducing the vibratory loads, a larger amount of 2/rev input is required to produce an amount of vibration reduction comparable to that associated with 3/rev, 4/rev and 5/rev components, which despite their small amplitudes, are much more effective in reducing vibration levels. Therefore, while the MFPC signal in the rotating frame appears to consist of a predominantly 2/rev signal, in reality much of the vibration reduction is achieved by 3/rev, 4/rev and 5/rev components which are not clearly visible because they are overshadowed by the 2/rev component, due to their relatively small magnitude. For this reason the physical explanation given in Refs. 17-19, attempting to rationalize the importance of the 2/rev component is incorrect and misleading. Fortunately we persevered and found the correct explanation, which provides useful insight into the reduction of vibration levels using high frequency pitch control in the rotating frame.

6.3 Comparison of vibration reduction schemes with control vectors $\{\theta_E\}$ and $\{\theta_R\}$

The problem of simultaneous reduction of hub shears and fuselage accelerations was solved in Section 5.2 following the minimum variance controller approach. In this section, the MFPC signal represented by the control vector $\{\theta_R\}$ is introduced to the coupled rotor/flexible fuselage system and the vibration reduction achieved is compared with that obtained when using the the control vector $\{\theta_E\}$. For convenience, this study is based on the offset hinged spring restrained blade model. The fuselage is assumed to be very stiff in lateral bending and torsion; however the fundamental frequency in vertical bending is assumed to be 4/rev. The calculations are performed for an advance ratio $\mu = 0.3$

Figure 9 depicts MFPC variation in the rotating frame corresponding to the two control pitch input vectors $\{\theta_E\}$ and $\{\theta_R\}$, respectively; as well as their harmonic components. It is interesting to note that for the example considered, for simultaneous reduction of hub loads and fuselage accelerations, both control vectors $\{\theta_E\}$ and $\{\theta_R\}$ provide almost identical pitch variation in the rotating frame. This result indicates that for the example problem the control vectors converged to the same MFPC signal in the rotating frame while achieving the desired reduction in the vibratory response.

Figure 10 shows the baseline peak-to-peak vibratory hub shears, hub moments and the accelerations at the C.G. of the fuselage together with the controlled vibratory levels. Both approaches, namely vibration control with either the control vector $\{\theta_E\}$ or $\{\theta_R\}$, provided a very good reduction in the hub loads and C.G. accelerations. The vibratory hub moments obtained with minimum variance controller, Eq. (37), which in Fig. 10 is denoted optimal control is almost equal to that obtained with the control vector having a frequency combination of $\overline{\omega}_{HH} = 3$/rev and 4/rev. Note that these results were obtained with global controller which is equivalent to the local controller with one iteration.

6.4 Influence of fuselage flexibility on the vibration reduction scheme

Recall that the vibration reduction studies were conducted with a flexible fuselage which allowed only vertical bending. Very high stiffnesses in lateral bending and torsion were used to effectively suppress these two elastic degrees of freedom. In this section, the fuselage stiffnesses in lateral bending and in torsion are reduced so as to study the effect of fuselage flexibility on the vibration reduction using open loop pitch control. For this case the fundamental frequency in vertical bending of the fuselage is $\omega_{BV1} = 4.0$/rev; in horizontal bending $\omega_{BH1} = 4.0$/rev and the fundamental torsional frequency is $\omega_{T1} = 3.5$/rev . This represents an unfavorable fuselage frequency placement which can be easily excited by a four bladed rotor system.

The approach used for simultaneous reduction of hub loads and the fuselage accelerations is based on the minimum variance control algorithm, utilizing the control vector $\{\theta_R\}$. This approach was selected because it has a sound mathematical basis.

Figure 11 depicts the MFPC input in the rotating frame together with its harmonic content. Again the control signal is predominantly 2/rev with additional harmonic content consisting of: about 5% in 3/rev, 2% in 4/rev and 11% in 5/rev.

The effect of this control signal on the peak-to-peak hub loads and fuselage accelerations is shown in Fig. 12. While all the inplane hub shears show a substantial

reduction, the reduction in vertical hub shear is only marginal. The roll moment has increased by a factor of three from its baseline value. The acceleration levels at the C.G. showed a reduction in the Y-direction (ACY); but the acceleration in vertical direction (ACZ) has increased. This result indicates that a simultaneous reduction in all the components hub loads and the C.G. accelerations was not possible. The reason for the increase in some components of the vibratory loads can be explained by analyzing the harmonic contents of the vibratory hub loads and C.G. accelerations.

The harmonic components of the hub loads and accelerations is given in Table 5. It can be seen from this Table that the 4/rev content of the hub shears in all directions is reduced;however the 8/rev content of the hub shears exhibits a substantial increase. Recall that in this case the performance index consists only of the 4/rev contents of the hub shears and C.G. accelerations. Since the 8/rev contents of the loads is essentially uncontrolled, these components are influenced by the introduction of a higher harmonic MFPC control pitch input in the rotating frame.

7. Concluding Remarks

This paper describes an attempt to develop a multi frequency pitch control (MFPC) technique, which can produce simultaneous reduction of hub shears and fuselage accelerations in a coupled rotor/flexible fuselage helicopter model. Two types of control vectors were used in minimizing the vibratory hub loads and fuselage accelerations. The influence of fuselage flexibility on the effectiveness of the MFPC control pitch input was also studied. The most interesting conclusions obtained are summarized below.

(1) When the fuselage flexibility was limited to vertical bending only , (and the lateral bending and torsion were essentially suppressed), the MFPC can reduce simultaneously the hub shears and fuselage C.G. accelerations.

(2) The shape of the MFPC signal in the rotating frame depends on the particular model used to represent the blade flexibility. When the offset hinged spring restrained blade model was used, the MFPC signal has substantial 2/rev content with 17% content in 3/rev and a 4% content in 4/rev. For the fully elastic blade model, the 2/rev content in MFPC signal was reduced, however it still was the largest component with 30% content in 3/rev and about 10% to 20% content in 4/rev and 5/rev.

(3) A careful sensitivity analysis conducted revealed that the introduction of a single frequency pitch input with a frequency 2,3,4 or 5/rev in the rotating frame is capable of reducing the vibratory hub shears. For the four bladed rotor system, the vertical hub shear reduction required a pitch angle whose amplitude is highest for 2/rev pitch input and lowest for 4/rev pitch input in the rotating frame. When considering the the sensitivity of the hub shears to single frequency pitch input in the rotating frame, the 4/rev vertical hub shear is least sensitive to 2/rev pitch input; highly sensitive to 4/rev pitch input;and moderately sensitive to 3/rev and 5/rev pitch input.

A high sensitivity with respect to a particular harmonic (such as 4/rev for a four bladed rotor system) implies the need for a precise control of the pitch inputs. For harmonics which have a strong influence on the hub shears, the requirement of a

very small amplitude may be physically unrealizable in an actual vibration reduction device.

(4) The MFPC control signal obtained using two different control vectors, provided identical pitch angle variation in the rotating frame for simultaneous reduction of hub loads and C.G accelerations. This confirms that the error found in our previous studies, Refs. 17-19, has been corrected.

(5) Simultaneous reduction of all the components of hub shears and fuselage accelerations for a completely flexible fuselage, containing a broad frequency spectrum requires additional study.

APPENDIX A

Using the linear assumption, represented by Eq. (24) and expanding Eq. (41), the vertical vibratory hub shears can be written as:

$$F_{Hz4c} = F_{0Hz4c} + T_{CC}\, A \sin\phi + T_{CS}\, A \cos\phi$$

$$F_{Hz4s} = F_{0Hz4s} + T_{SC}\, A \sin\phi + T_{SS}\, A \cos\phi \qquad \text{(A.1)}$$

where F_{0Hz4c}, F_{0Hz4s} represent the baseline vetical hub shear components and the superscript p, in Eqs. (A.1) was deleted for the sake of convenience. For a linear system with time-invariant coefficients the [T] matrix has the following properties

$$T_{CC} = T_{SS} = T_a$$

$$T_{CS} = -T_{SC} = T_b \qquad \text{(A.2)}$$

which have been also noted in Ref. 23. For this case it can be shown that the minimum peak to peak vertical hub shear will be zero when the amplitude of the pitch input is equal to

$$A\ \min = \left[\frac{(F_{0z4c})^2 + (F_{0z4s})^2}{(T_a)^2 + (T_b)^2} \right]^{\frac{1}{2}} \qquad \text{(A.3)}$$

and the minimum peak to peak vertical hub shear will be equal to the baseline value when the amplitude of the input is equal to 2 A min. If the computer code is used to calculate the coefficients T_{CC}, T_{CS}, T_{SC} and T_{SS} by a finite difference approach, such as the one employed for calculating the elements of the T matrix in Section 5, the property depicted by Eqs. (A.2) will be only approximately valid. This is due to the nonlinearity in the equations as well as the periodic coefficients associated with forward flight [23]. It is therefore possible to obtain approximate values for T_a, T_b in Eqs. (A.2) by averaging the coefficients

$$T_a = \frac{1}{2}(T_{CC} + T_{SS})$$

$$T_b = \frac{1}{2}(T_{CS} - T_{SC}) \tag{A.4}$$

These approximate values for T_a and T_b are used in Eq. (A.3) to obtain approximate values for A min.

APPENDIX B

The equation of motion for a centrally hinged spring restrained rigid blade undergoing flapping motion, in forward flight can be written as

$$\ddot{\beta} + \gamma\left\{\frac{1}{8} + \frac{\mu}{6}\sin\psi\right\}\dot{\beta} + \left\{1 + \bar{\omega}_F^2 + \gamma\left(\frac{\mu}{6}\cos\psi + \frac{\mu^2}{4}\sin\psi\cos\psi\right)\right\}\beta =$$

$$\gamma\left\{\left(\frac{1}{8} + \frac{\mu}{3}\sin\psi + \frac{\mu^2}{4}\sin^2\psi\right)\theta + b\left(\frac{1}{6} + \frac{\mu}{4}\sin\psi\right)\dot{\theta}\right.$$

$$\left. - \lambda\left(\frac{1}{6} + \frac{\mu}{4}\sin\psi\right)\right\} \tag{B.1}$$

In Eq. (B.1), the terms associated with noncirculatory lift are not considered, reverse flow effects have been neglected and the inflow is assumed to be uniform. Equation (B.1) is obtained after simplifying the more general rotor blade equations derived in Ref. 25. The blade root shear in the vertical direction, also from Ref. 25, can be written as

$$F_Z = \frac{\sigma a}{2N_b}\left\{\left(\frac{1}{3} + \frac{\mu^2}{2} + \mu\sin\psi - \frac{\mu^2}{2}\cos 2\psi\right)\theta -\right.$$

$$\left(\frac{1}{2} + \mu\sin\psi\right)\lambda - \left(\frac{1}{3} + \frac{\mu}{2}\sin\psi\right)\dot{\beta} +$$

$$\left. b\left(\frac{1}{3} + \mu\sin\psi\right)\dot{\theta} - \left(\frac{\mu}{2}\cos\psi + \frac{\mu^2}{2}\sin 2\psi\right)\beta\right\} \tag{B.2}$$

The blade root shear is nondimensionalized with respect to $\bar{\rho}\pi\bar{R}^2(\overline{\Omega R})^2$.

Assuming that θ and β consist of five harmonics (including a constant term) and substituting these harmonic expansions for β and θ in Eq. (B.2) yields the blade root shear in the vertical direction as a function of harmonics of flap response and pitch input.

For a four bladed rotor, the hub vertical shear can be obtained by summing up Eq. (B.2) for four blades. The resulting 4/rev vertical hub shear, in terms of higher harmonic blade pitch input and higher harmonic flap response, can be written as

$$F_{Hz4} = \frac{\sigma a}{2}\Bigg[\cos 4\psi \Bigg\{ -\frac{\mu^2}{4}\theta_C^2 - \frac{\mu}{2}\theta_S^3 + \frac{3}{2}b\mu\theta_C^3 + \left(\frac{1}{3}+\frac{\mu^2}{2}\right)\theta_C^4 + 2b\theta_C^4 + \frac{\mu}{2}\theta_S^5 - \frac{5}{2}b\mu\theta_C^5 + \frac{\mu^2}{4}\beta_{2S} - \mu\beta_{3C} - \frac{4}{3}\beta_{4S} - \frac{\mu}{4}\beta_{5C}\Bigg\} + \sin 4\psi \Bigg\{ -\frac{\mu^2}{4}\theta_S^2 + \frac{\mu}{2}\theta_C^3 + \frac{3}{2}b\mu\theta_S^3 + \left(\frac{1}{3}+\frac{\mu^2}{2}\right)\theta_S^4 - 2b\theta_C^4 - \frac{\mu}{2}\theta_C^5 - \frac{5}{2}b\mu\theta_S^5 - \frac{\mu^2}{4}\beta_{2C} - \mu\beta_{3S} + \frac{4}{3}\beta_{4C} - \frac{\mu}{4}\beta_{5S}\Bigg\}\Bigg] \qquad \text{(B.3)}$$

From Eq. (B.3), it is evident that the 4/rev hub shear is least affected by the 2/rev pitch input and the 2/rev blade response because these terms are multiplied by μ^2 , and therefore for advance ratios of $\mu < 0.4$ these terms will be significantly smaller than the other terms. On the other hand, the 3/rev and 5/rev pitch inputs are multiplied by μ ; and the 4/rev pitch inputs are multiplied by the term $1/3 + \mu^2/2$. The relative orders of magnitude of the coefficients of the harmonics of the pitch input and flap response clearly indicate that the 4/rev vertical hub shear is most sensitive to 4/rev harmonics, moderately sensitive to 3/rev and 5/rev harmonics and least sensitive to 2/rev harmonics of the pitch input in the rotating frame.

Aknowledgements

This research was funded by NASA Ames Research Center under grant NAG2-477, the useful comments of the grant monitor Dr. S. Jacklin are gratefully acknowledged.

REFERENCES

1. Reichert, G. , " Helicopter Vibration Control-A Survey," Vertica , Vol 5, No 1, pp 1-20, 1981.

2. Loewy, R.G., "Helicopter Vibrations : A Technological Perspective," AHS Journal , Vol. 29, No. 4, October 1984, pp.4-30.

3. Ham, N., "Helicopter Individual-Blade-Control and Its Applications," 39th AHS Forum, St. Louis, Missouri, May 1983.

4. Richer, P., Eisbrecher, H.D. and Kloppel, V., " Design and Flight Tests of Individual Blade Control Actuators," Proceedings of the 16th European Rotorcraft Forum, Glasgow, U.K., Sept. 18-21, 1990, pp. III.6.3.1-III.6.3.9

5. Taylor, R.B., Farrar, F.A., and Miao, W., " An Active Control System for Helicopter Vibration Reduction by Higher Harmonic Pitch," AIAA Paper No. 80-0672, 36th AHS Forum, Washington D.C., May 1980.

6. Molusis, J.A., " The Importance of Nonlinearity on the Higher Harmonic Control of Helicopter Vibration," 39th AHS Forum, St. Louis, Missouri, May 1983.

7. Chopra, I., and J.L. McCloud, "A Numerical Simulation Study of Open-Loop, Closed-Loop and Adaptive Multicyclic Control Systems," AHS Journal, Vol. 28, No. 1, January 1983, pp. 63-77.

8. Robinson, L., and Friedmann, P.P., " Analytic Simulation of Higher Harmonic Control Using a New Aeroelastic Model," Proc. 30th AIAA/ASME/ASCE/AHS/ACS Structures, Structural Dynamics and Materials Conference, Mobile, Alabama, April 1989. AIAA Paper No. 89.1321.

9. Robinson, L., and Friedmann, P.P., " A Study of Fundamental Issues in Higher Harmonic Control Using Aeroelastic Simulation," AHS Journal, Vol. 36, No. 2, April 1991, pp. 32-43.

10. Nguyen, K. and Chopra, I., "Application of Higher Harmonic Control (HHC) to Rotors Operating at High Speed and Maneuvering Flight," Proceedings of the 45th Annual Forum of the American Helicopter Society, Boston, MA, May 1989, pp 81-96.

11. Molusis, J.A., Hammond, C.E., and Cline, J.H., "A Unified Approach to the Optimal Design of Adaptive and Gain Scheduled Controllers to Achieve Minimum Helicopter Vibration," AHS Journal , Vol.28, No.2, April 1983, pp. 9-18.

12. Lehmann, G., " The Effect of Higher Harmonic Control (HHC) on a Four-Bladed Hingeless Model Rotor," Vertica , Vol.9, No.3, 1985, pp. 273-284.

13. Shaw, J., Albion, A., Hanker, E.J., and Teal, R., "Higher Harmonic Control: Wind Tunnel Demonstration of Fully Effective Vibratory Hub Force Suppression," AHS Journal , Vol.34, No.1, January 1989, pp. 14-25.

14. Wood, E.R., Powers, J.H., Cline, J.H., and Hammomd, C.E., "On Developing and Flight Testing a Higher Harmonic Control System," AHS Journal , Vol.30, No.1, January 1985, pp. 3-20.

15. Miao, W., and Frye, H.M., "Flight Demonstration of Higher Harmonic Control (HHC) on S-76," 42nd AHS Forum, Washington, D.C., June 1986.

16. Polychroniadis, M., and Achache, M., "Higher Harmonic Control: Flight Tests of an Experimental System on SA 349 Research Gazelle," 42nd AHS Forum, Washington, D.C., June 1986.

17. Papavassiliou ,I., Venkatesan, C. and Friedmann, P.P., " A Study of Coupled Rotor-Fuselage Vibration with Higher Harmonic Control Using a Symbolic Computing Facility," Proceedings of the 16th European Rotorcraft forum, Glasgow U.K., Sept. 18-21, 1990, pp. III.7.3.1-III.7.3.23

18. Papavassiliou, I., " Nonlinear Coupled Rotor/Fuselage Vibration Analysis and Higher Harmonic Control Studies for Vibration Reduction in Helicopters," Ph.D. Dissertation, Mechanical, Aerospace and Nuclear Engineering Department, University of California, Los Angeles, January 1991.

19. I. Papavassiliou, P. P. Friedmann and C. Venkatesan, "Coupled Rotor-Flexible Fuselage Vibration Reduction Using Open Loop Higher Harmonic Control," AIAA Paper No. 91-1217, Proceedings of the 32nd AIAA/ASME/ASCE/AHS/ACS Structures, Structural Dynamics and Materials Conference, Baltimore, Maryland, April 8-10, 1991, pp. 2011-2035.

20. Stephens, W.B. and Peters, D.A., "Rotor-Body Coupling Revisited," AHS Journal , Vol. 32, No. 1, January 1987, pp. 68-72.

21. Takahashi, M.D. and Friedmann, P.P., " Active Control of Helicopter Helicopter Air Resonance in Hover and Forward Flight," AIAA Paper 88-2407-CP, Procedings AIAA/ASME/ASCE/AHS 29th Structures, Structural Dynamics and Material Conference, Williamsburg VA, April 1988, pp 1521-1532.

22. Takahashi, M.D., " Active Control of Helicopter Aeromechanical and Aeroelastic Instabilities," Ph.D. Dissertation, Mechanical Aerospace and Nuclear Engineering Department, University of California, Los Angeles, June 1988.

23. Johnson, W., "Self Tuning Regulators for Multicyclic Control of Helicopter Vibration," NASA TP 1996, 1982

24. Davis, M.E., "Refinement and Evaluation of Helicopter Real-Time Self-Adaptive Active Vibration Controller Algorithms," NASA CR 3821, August 1984.

25. Venkatesan C., and Friedmann, P., "Aeroelasic Effects in Multi-Rotor Vehicles with Applications to a Heavy-Lift System, Part 1 : Formulation of Equations of Motion," NASA-CR 3822, August 1984.

TABLE 1

Data for coupled rotor/fuselage model used for offset hinged spring restrained blade configuration

Rotor Data	
$\mu = 0.3$	$a = 5.7$
$e = 0.0$	$C_{d0} = .01$
$\gamma = 5.0$	$N_b = 4$
$\sigma = .05$	$\theta_T = 0$ rad
$\omega_{F1} = 1.15$	$C_x = .0$
$\omega_{L1} = 0.57$	$C_y = .0$
$\omega_{T1} = 4.5$	$C_z = .0$
Fuselage Data	
$l_F = 1.$	$C_w = 0.005$
$X_{MH}/l_F = .196$	$X_{MC}/l_F = .196$
$Z_{MH}/l_F = .233$	$Z_{MC}/l_F = 0.0$
$X_{MA}/l_F = .196$	$Z_{MA}/l_F = 0.0$

TABLE 2

Data for the coupled rotor/fuselage model used for the elastic blade configuration

Rotor Data	
μ = variable	$a = 2\pi$
$e = 0.0$	$C_{d0} = .01$
$\gamma = 5.5$	$N_b = 4$
$\sigma = .07$	$\theta_T = 0$ rad
$\omega_F = 1.123,3.41,7.65$	$C_x = .0$
$\omega_L = 0.735,4.485$	$C_y = .0$
$\omega_T = 3.17$	$C_z = .0$
Fuselage Data	
$l_F = 2.$	$C_w = 0.005$
$X_{MH}/l_F = .3$	$X_{MC}/l_F = .3$
$Z_{MH}/l_F = .15$	$Z_{MC}/l_F = 0.0$
$X_{MA}/l_F = .3$	$Z_{MA}/l_F = 0.0$

TABLE 3

Iteration history of peak to peak hub loads and C.G. accelerations for 3 and 4/rev MFPC combination using offset hinged blade model (local MFPC).

	Baseline	ITER. #1	ITER. #2	ITER.#3
Hub Forces (Nt)				
FHX	317.2	27.5	1.36	1.22
FHY	301.8	27.5	1.08	0.86
FHZ	1508.8	61.1	6.67	2.03
Hub Moments (Nt.m)				
MHX	536.5	150.5	96.99	99.90
MHY	506.5	31.6	1.26	0.96
C.G. Accelerations (g)				
ACX	3.9*1E-3	3.4*1E-4	1.6*1E-5	1.5*1E-5
ACY	3.7*1E-3	3.4*1E-4	1.2*1E-5	1.2*1E-5
ACZ	1.463	0.0171	0.0051	0.0038

TABLE 4

Iteration history of peak to peak hub loads and C.G. accelerations for 3 and 4/rev MFPC combination for the elastic blade model(local MFPC).

	Baseline	ITER. #1	ITER. #2	ITER.#3
Hub Forces (Nt)				
FHX	448.8	244.3	99.2	45.3
FHY	1258.8	362.1	147.8	98.3
FHZ	3615.0	318.2	147.5	61.0
Hub Moments (Nt.m)				
MHX	3184.4	4108.0	781.6	1091.1
MHY	2881.0	3444.0	612.6	417.1
C.G. Accelerations (g)				
ACX	5.9*1E-3	4.1*1E-4	6.7*1E-4	1.2*1E-4
ACY	1.6*1E-2	3.6*1E-3	1.3*1E-4	1.6*1E-4
ACZ	7.731	0.485	0.24	0.0039

TABLE 5

Hub shears, hub moments C.G accelerations for the MFPC scheme with the offset hinged blade model and fully flexible fuselage.

		Baseline	with MFPC
Hub Forces (Nt)			
FHX	4p amplitude	303.23	44.48
	8p amplitude	0.23	19.04
	peak-to-peak	603.06	103.59
FHY	4p amplitude	497.45	197.36
	8p amplitude	0.16	18.32
	peak-to-peak	989.18	400.34
FHZ	4p amplitude	52.81	24.95
	8p amplitude	0.31	25.72
	peak-to-peak	104.97	86.97
Hub Moments (Nt*m)			
MHX	4p amplitude	443.16	1700.97
	8p amplitude	0.06	14.36
	peak-to-peak	877.50	3370.39
MHY	4p amplitude	411.62	67.23
	8p amplitude	0.07	14.08
	peak-to-peak	818.40	141.74
C.G. Accelerations (g)			
ACX	4p amplitude	0.37*1E-2	0.54*1E-3
	8p amplitude	0.28*1E-5	0.23*1E-3
	peak-to-peak	7.35*1E-3	1.22*1E-3
ACY	4p amplitude	0.60137	0.14579
	8p amplitude	1.06*1E-5	0.62*1E-3
	peak-to-peak	1.19134	0.29107
ACZ	4p amplitude	0.14265	0.15892
	8p amplitude	2.24*1E-5	0.45*1E-3
	peak-to-peak	0.23701	0.31658

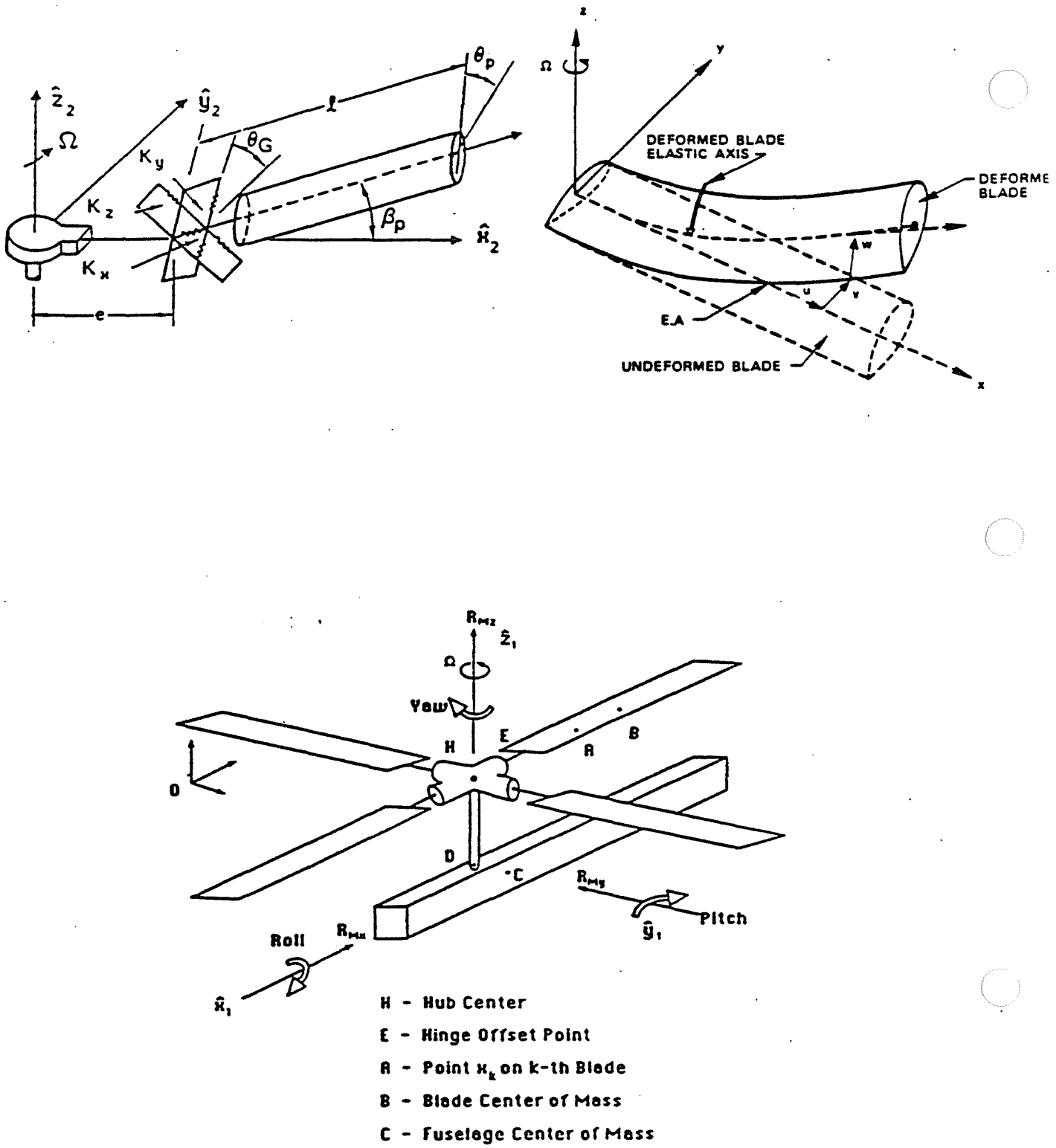

Figure 1: Coupled rotor/flexible fuselage model

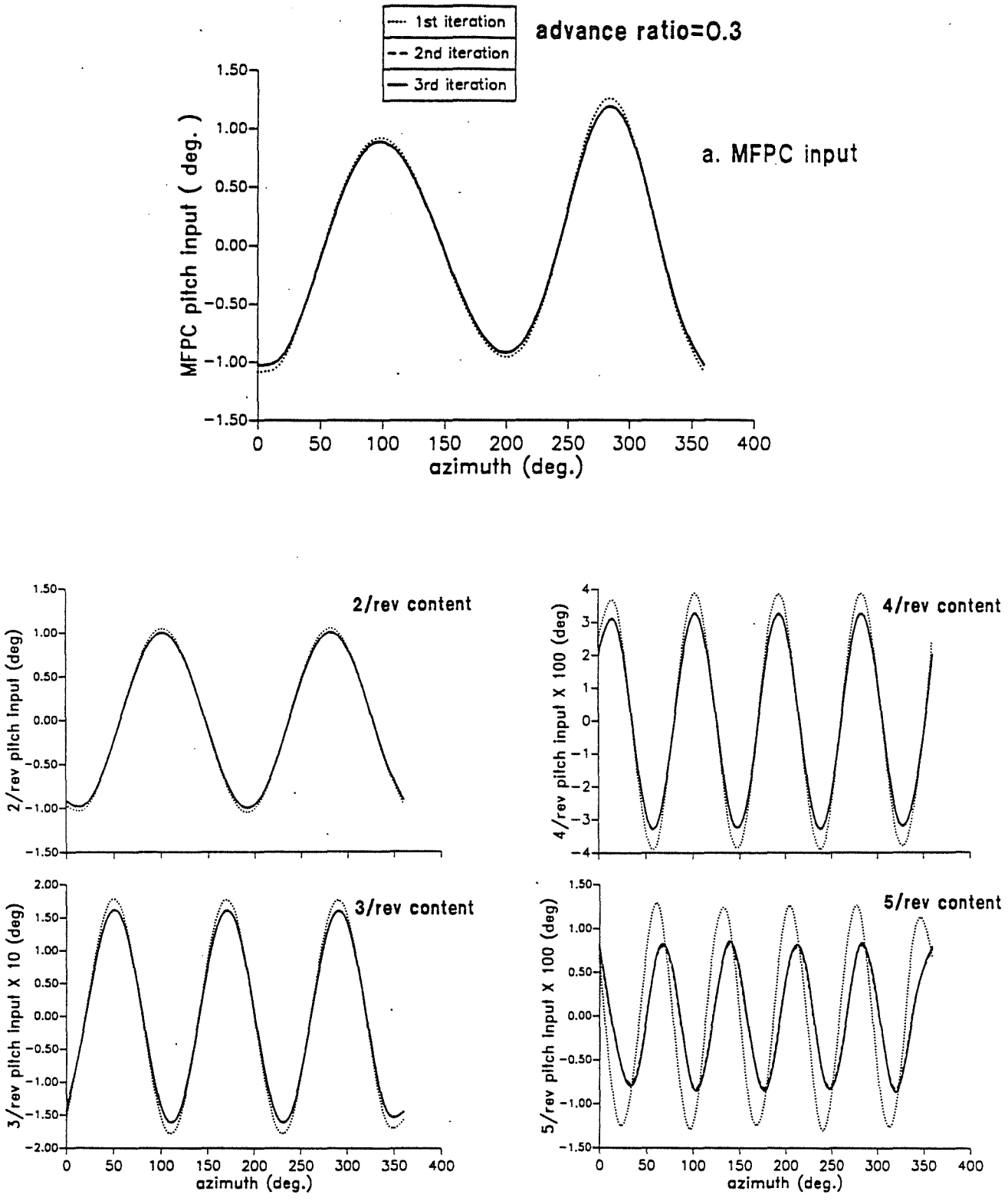

Figure 2: MFPC pitch angle variation in the rotating frame with 3 and 4/rev combination for the offset hinged blade configuration. Three iterations of the local MFPC model are shown. (a) MFPC pitch input (b) Harmonic contents of MFPC input

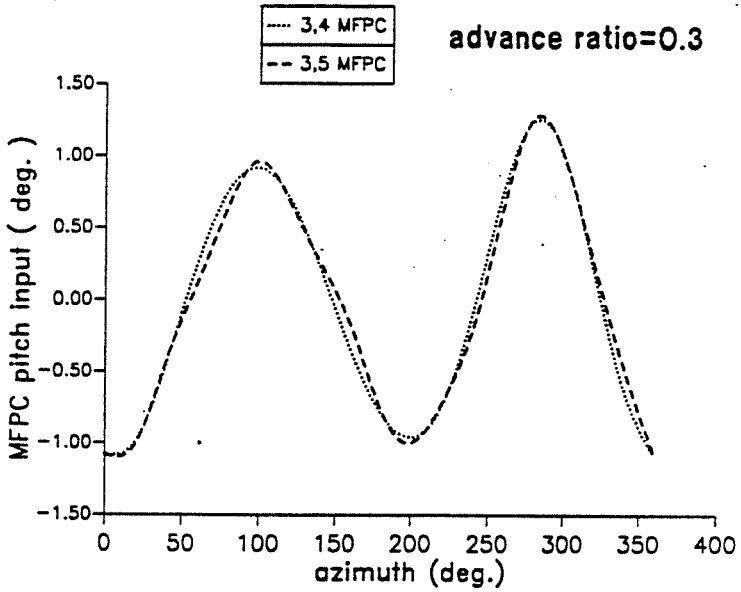

a. MFPC input

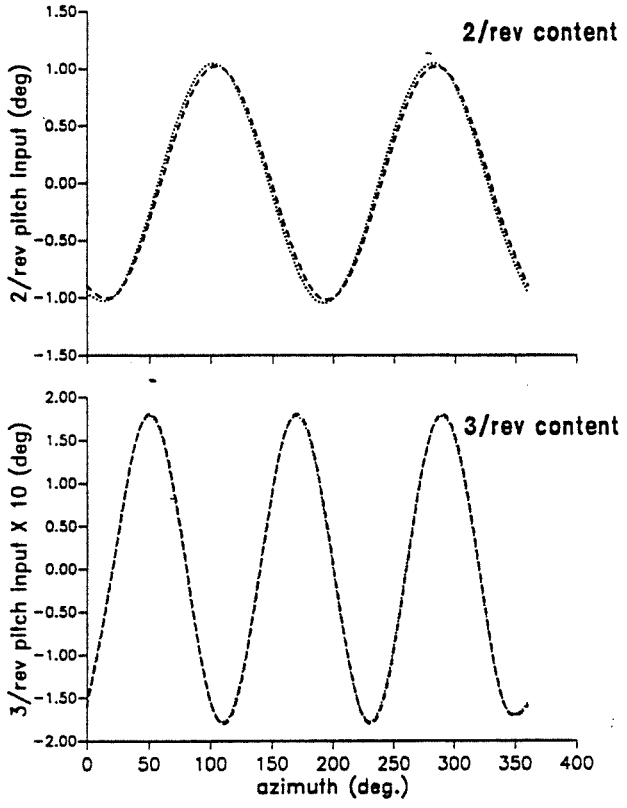

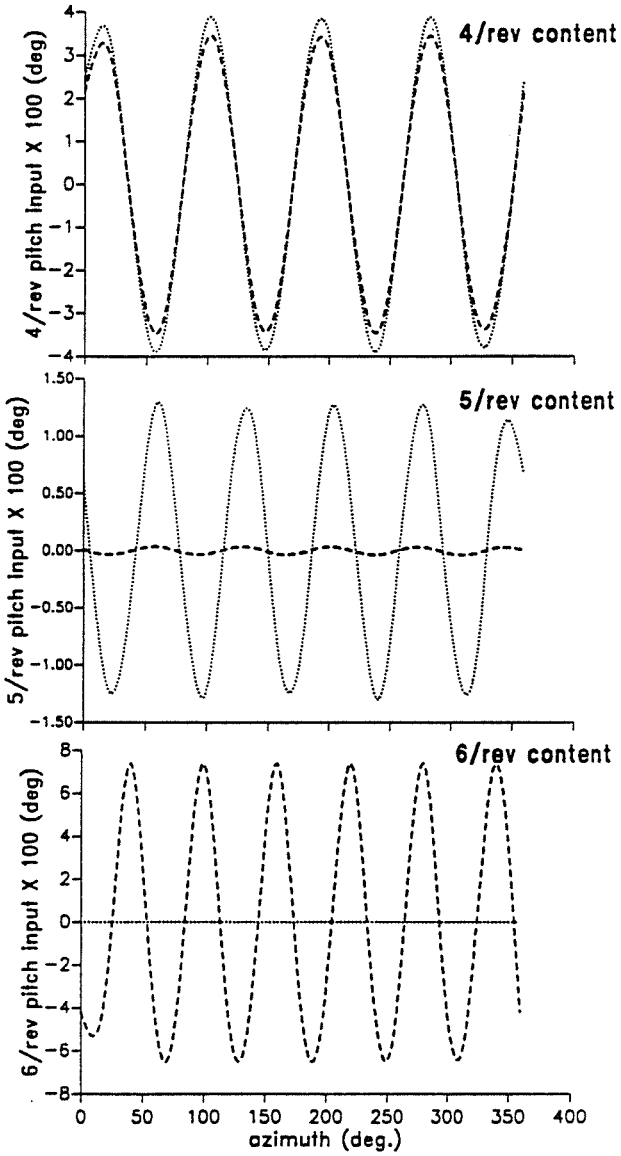

b. Harmonic contents of MFPC input

Figure 3: MFPC pitch angle variation in the rotating frame with 3 and 4/rev, 3 and 5/rev combinations for the offset hinged blade configuration and global MFPC model. (a) MFPC pitch input (b) Harmonic contents of MFPC input

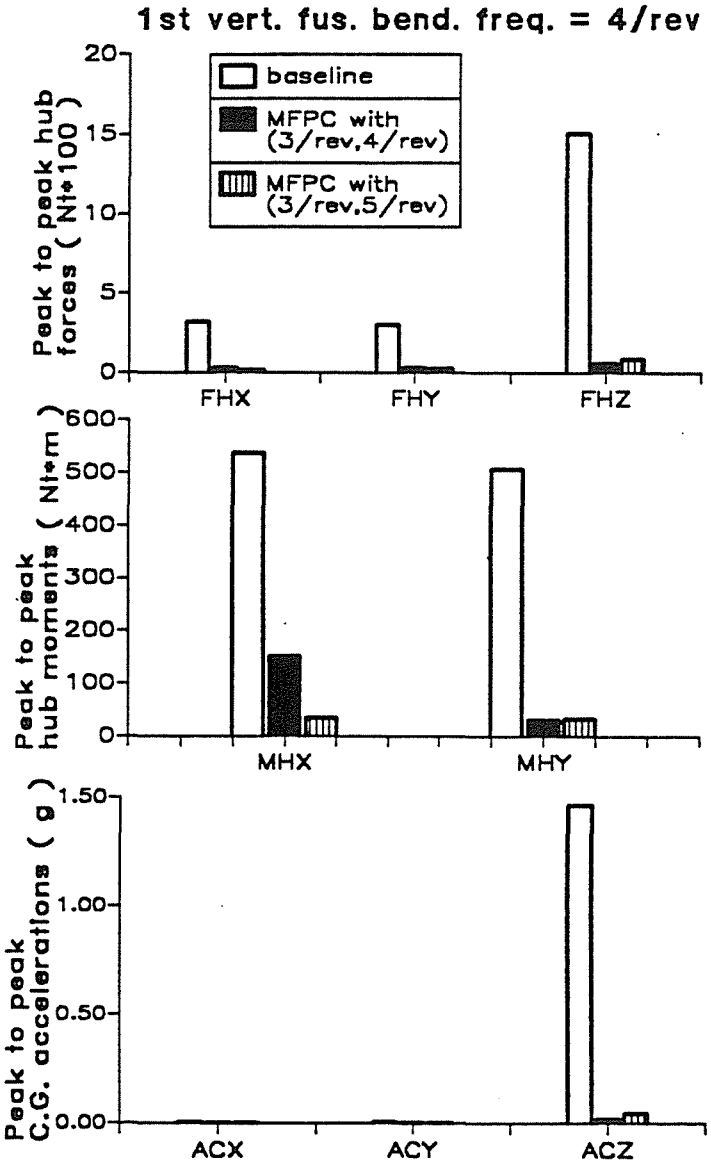

Figure 4: Hub shears, hub moments and fuselage C.G accelerations without MFPC and with 3 and 4/rev, 3 and 5/rev MFPC combinations for the offset hinged blade configuration and global MFPC model

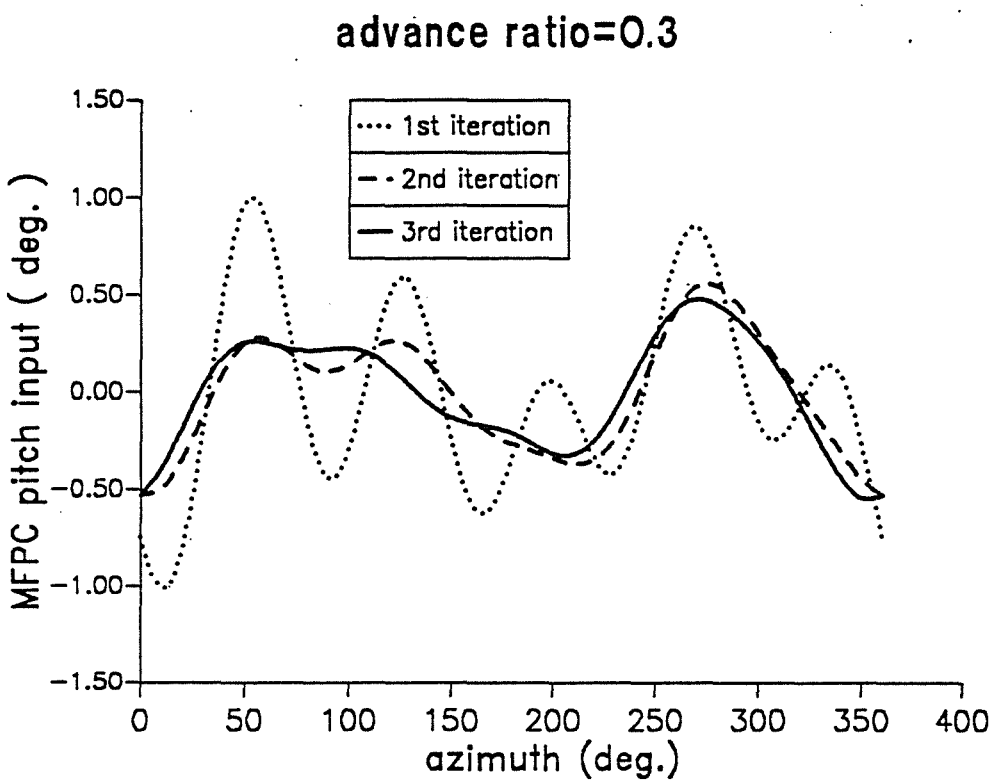

Figure 5: MFPC pitch angle variation in the rotating frame with 3,4/rev combination for the elastic blade model configuration. Three iterations of the local MFPC model are shown.

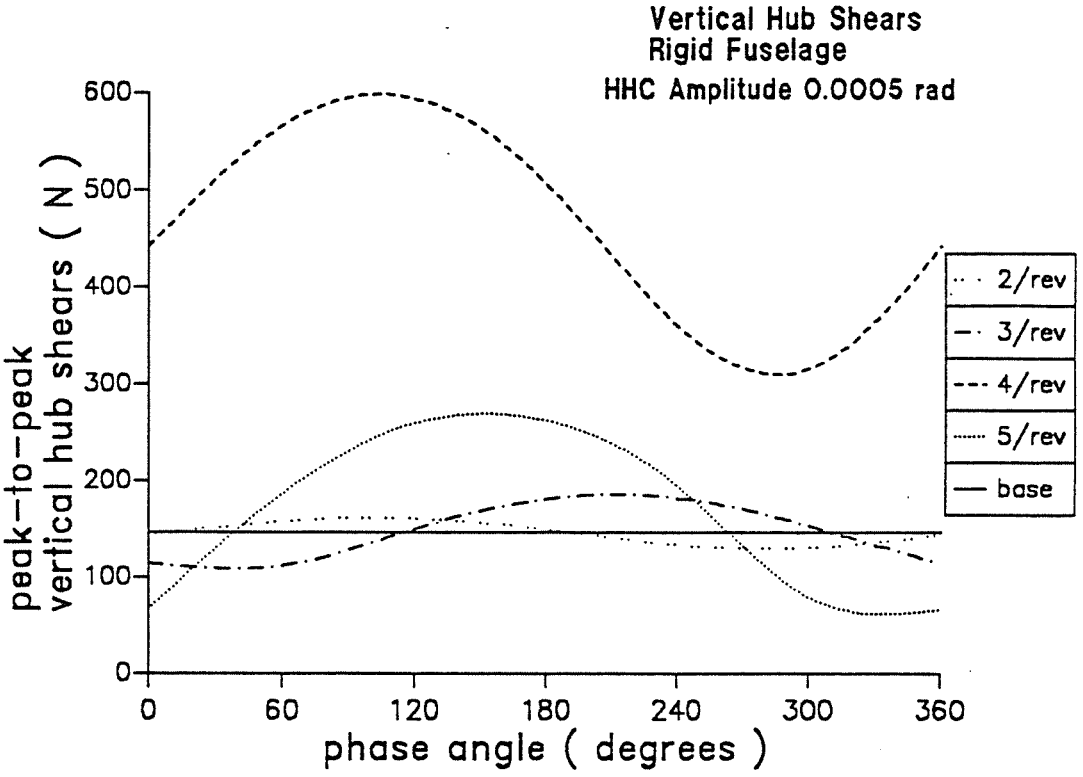

Figure 6: Influence of single frequency higher harmonic pitch inputs, in the rotating frame, on the vertical hub shear.

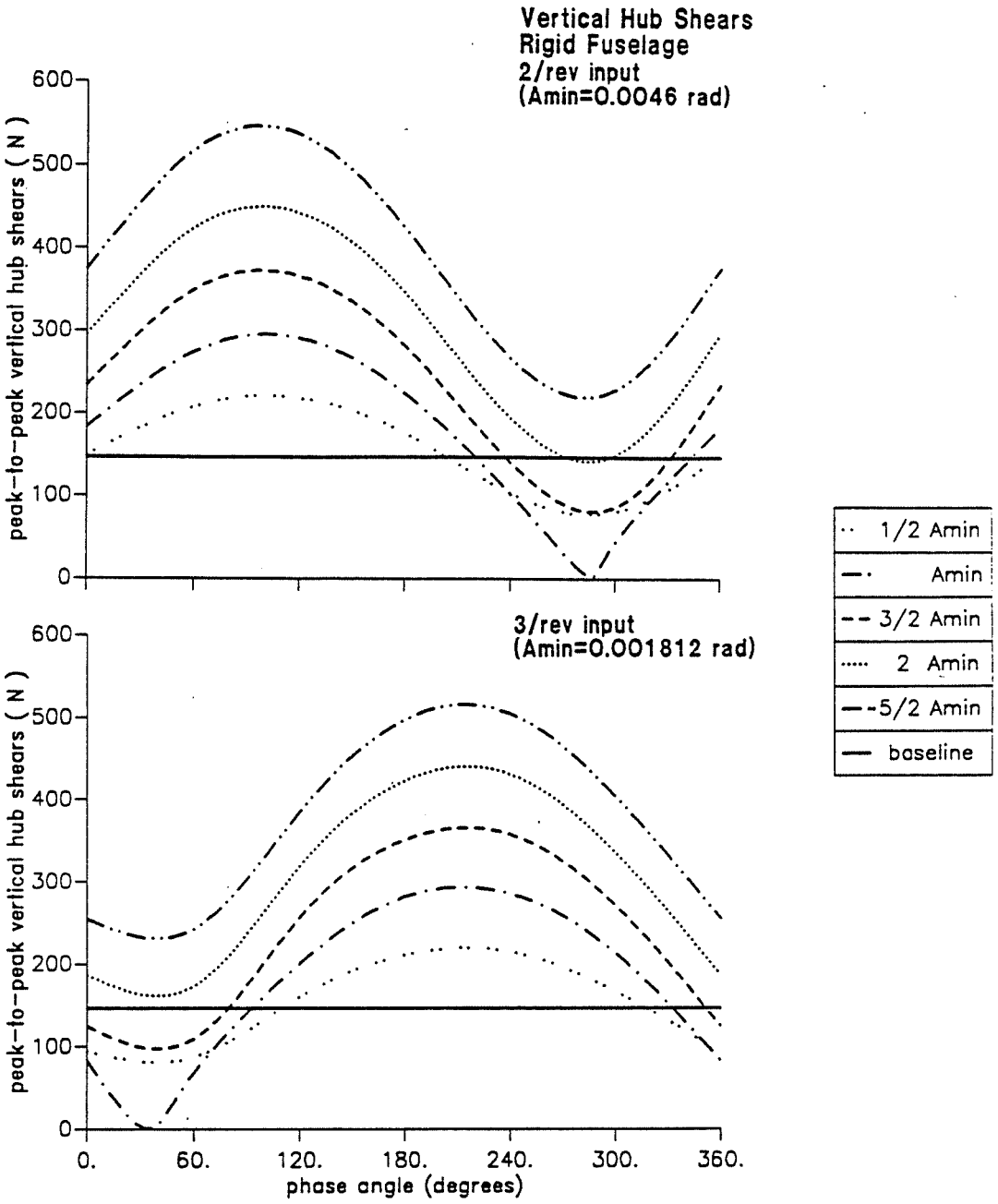

Figure 7: Influence of amplitude of 2/rev and 3/rev signals in the rotating frame, on the vertical hub shear.

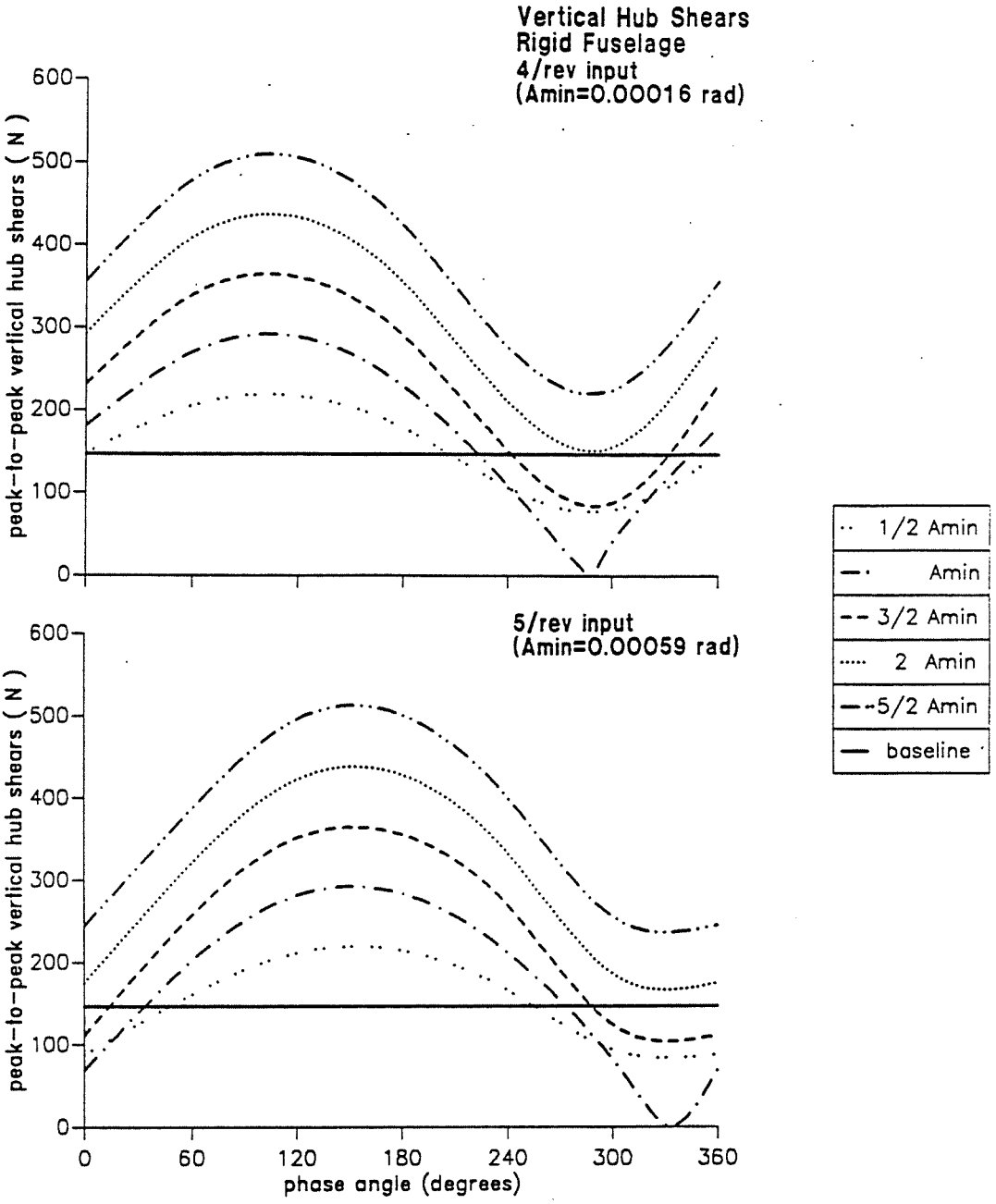

Figure 8: Influence of amplitude of 4/rev and 5/rev signals in the rotating frame, on the vertical hub shear.

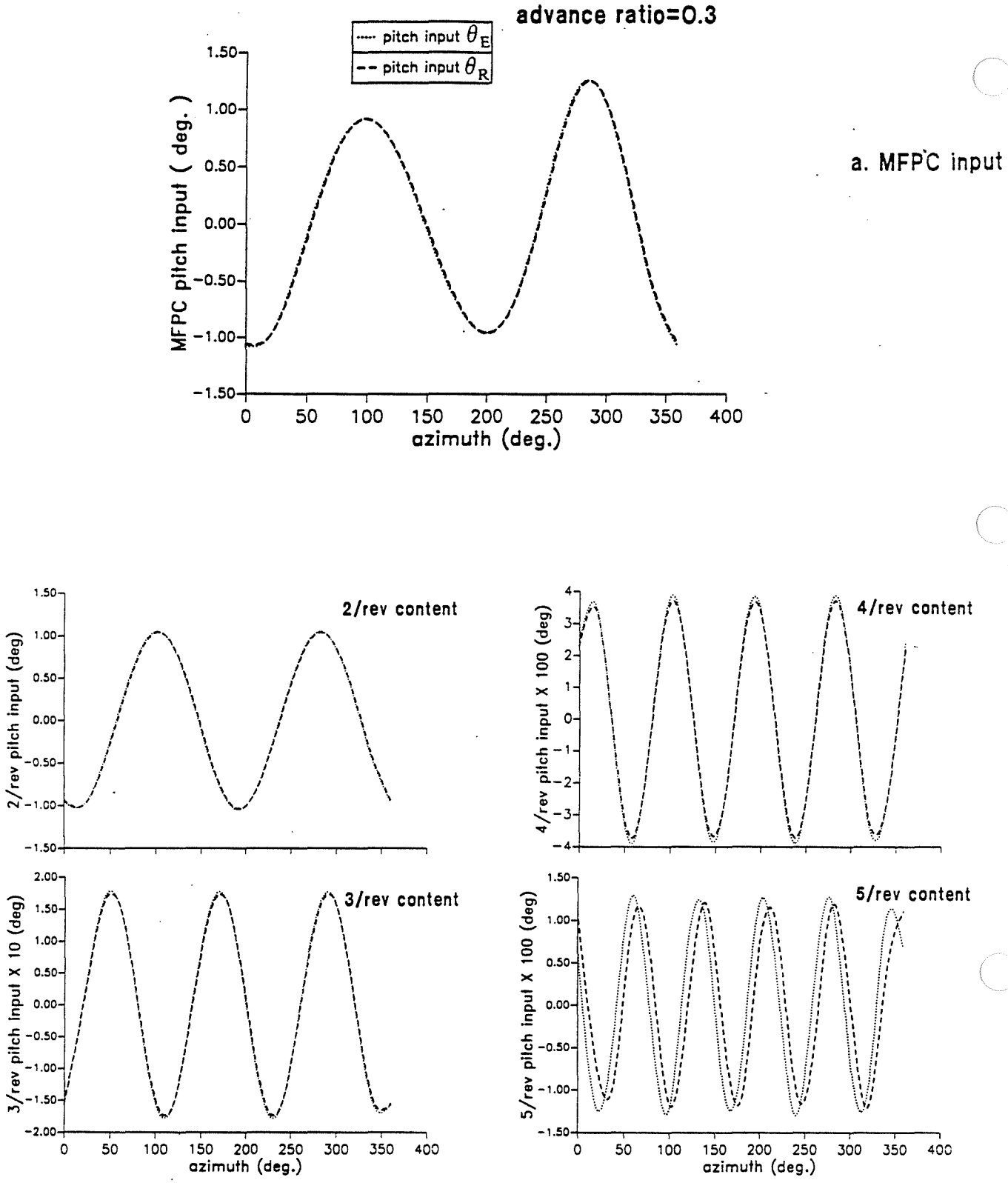

Figure 9: MFPC pitch angle variation in the rotating frame with pitch inputs $\{\theta_R\}$ and $\{\theta_E\}$ for the offset hinged blade configuration and global MFPC model. (a) MFPC pitch input (b) Harmonic contents of MFPC input

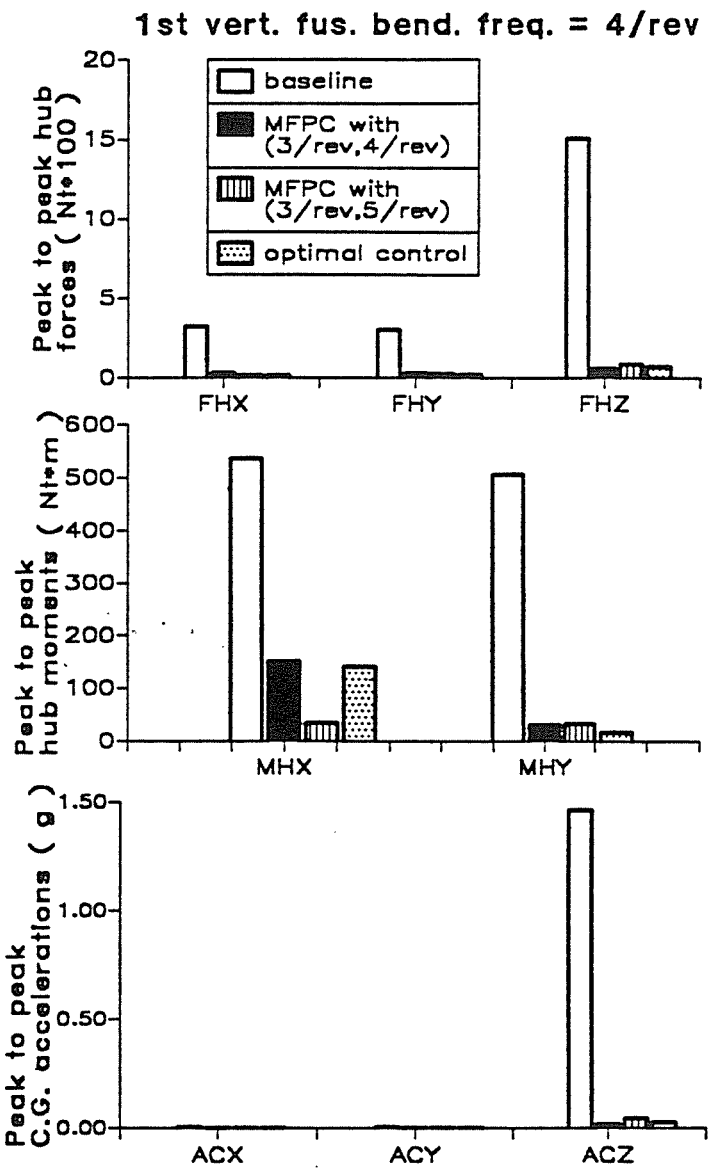

Figure 10: Hub shears, hub moments and fuselage C.G accelerations without MFPC and with various vibration reduction schemes for the offset hinged blade configuration.

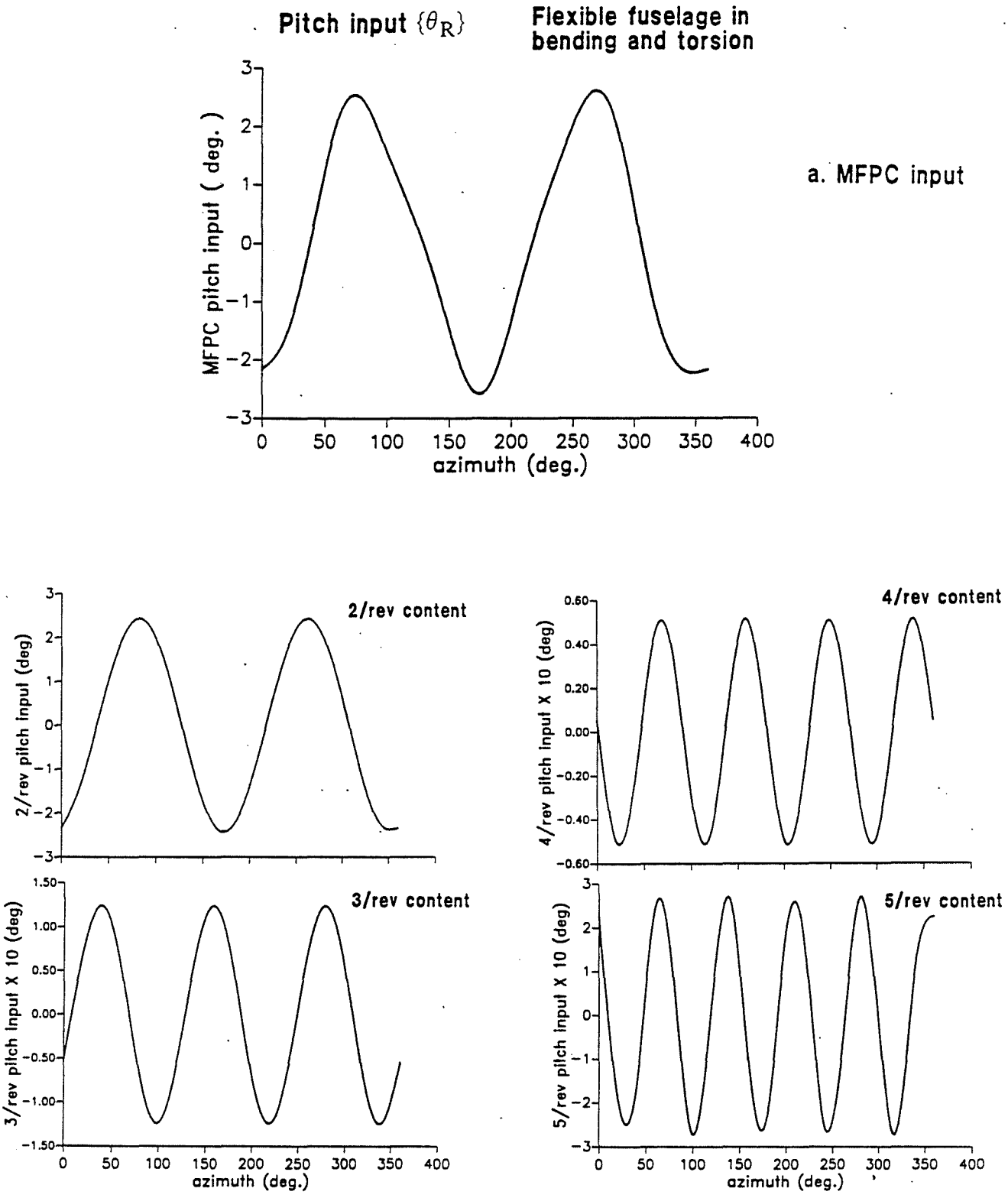

Figure 11: MFPC pitch angle variation in the rotating frame for a fully flexible fuselage. (a) MFPC pitch input (b) Harmonic contents of MFPC input

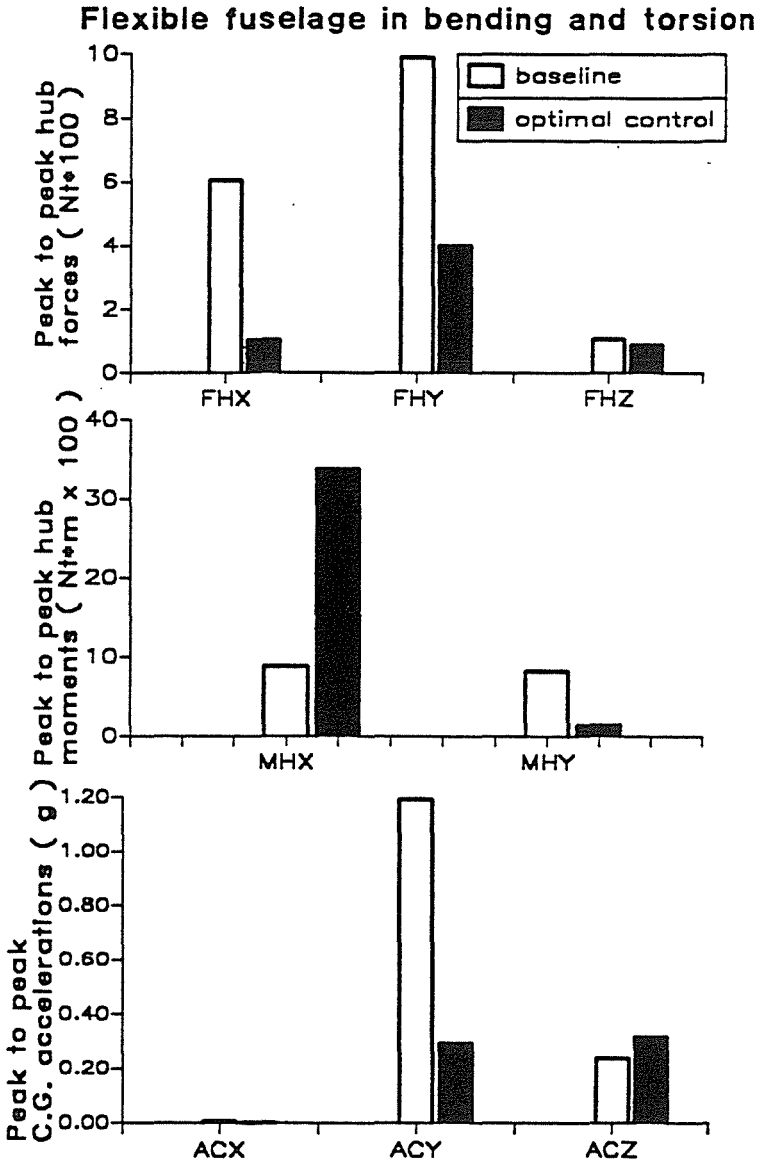

Figure 12: Hub shears, hub moments and fuselage C.G accelerations without MFPC and with minimum variance control input for a fully flexible fuselage.